JGR Biogeosciences

RESEARCH ARTICLE
10.1029/2022JG006908

Estimating Drivers and Pathways for Hydroelectric Reservoir Methane Emissions Using a New Mechanistic Model

Kyle B. Delwiche[1], John A. Harrison[2], Joannes D. Maasakkers[3], Melissa P. Sulprizio[4], John Worden[5], Daniel J. Jacob[4], and Elsie M. Sunderland[4]

[1]Department of Environmental Science, Policy, and Management, University of California, Berkeley, Berkeley, CA, USA, [2]School of the Environment, Washington State University, Vancouver, WA, USA, [3]SRON Netherlands Institute for Space Research, Leiden, The Netherlands, [4]School of Engineering and Applied Science, Harvard University, Cambridge, MA, USA, [5]Jet Propulsion Laboratory, California Institute for Technology, Pasadena, CA, USA

Key Points:

- Our mechanistic model (Reservoir Methane Emissions) illuminates the main drivers of hydropower methane emissions
- Emissions from downstream degassing are comparable to surface emissions when turbines are parameterized with deep water intakes
- We estimate global emissions from hydropower surfaces as 2.8 ± 0.2 Tg C/yr, plus 11 ± 4 Tg C/yr from downstream degassing

Supporting Information:

Supporting Information may be found in the online version of this article.

Correspondence to:

K. B. Delwiche,
kdelwiche@berkeley.edu

Citation:

Delwiche, K. B., Harrison, J. A., Maasakkers, J. D., Sulprizio, M. P., Worden, J., Jacob, D. J., & Sunderland, E. M. (2022). Estimating drivers and pathways for hydroelectric reservoir methane emissions using a new mechanistic model. *Journal of Geophysical Research: Biogeosciences*, *127*, e2022JG006908. https://doi.org/10.1029/2022JG006908

Received 17 MAR 2022
Accepted 2 AUG 2022

Abstract Hydroelectric reservoirs can emit significant quantities of methane, particularly through degassing at turbine outlets. Improved understanding of processes affecting hydroelectric reservoir CH_4 emissions is thus important as the world economy transitions to renewable forms of energy production. Here we develop and evaluate a new mechanistic model of CH_4 emissions: ResME ([**Res**]ervoir [**M**]ethane [**E**]missions), which estimates carbon inputs and methanogenesis to predict CH_4 release via ebullition and diffusion, plant emissions, and downstream emissions. ResME results demonstrate that the relative importance of allochthonous and autochthonous carbon input to methane emissions varies by latitude, with allochthonous carbon contributions typically being higher in tropical reservoirs. Results also demonstrate that total reservoir emissions are highly dependent on turbine intake depths, which are not typically reported. Potential maximum degassing emissions from existing hydroelectric reservoirs are estimated as 11 ± 4 Tg C/yr, if all reservoirs had deep turbine intakes and stratified for 5 months per year. In comparison, the estimated diffusive, ebullitive, and plant CH_4 emissions are estimated to be 2.8 ± 0.2 Tg C/yr (where the true uncertainty is much higher than the model standard error). Future work should focus on improving estimates of reservoir carbon inputs and decomposition rates, as well as surveying turbine intake depths. Satellite measurements from missions such as TROPOMI may also help constrain hydropower methane emissions.

Plain Language Summary Methane is an important greenhouse gas that is naturally produced in lake and reservoir sediment, among other sources. Hydroelectric power reservoirs produce renewable energy, yet also emit methane at their surfaces, and from turbines and downstream reaches. To better understand drivers and pathways of methane emissions, we have developed a new mechanistic model for methane emissions as a function of carbon inputs, chemical decomposition, and physical processes. Results also show that downstream methane emissions have the potential to exceed surface emissions if turbines pull from stratified, anoxic waters. Large uncertainties remain in model inputs, and future work should focus on improved understanding of carbon loading to reservoirs, as well as decomposition rates and turbine intake depths.

1. Introduction

Hydroelectric power is the dominant source of renewable energy globally. In 2017, it comprised 13% of global electricity production in OECD (Organization for Economic Co-operation and Development) countries (International Energy Agency, 2018), and 2.5% of global energy production. While electricity from hydropower can replace electricity from carbon-intensive sources such as coal and gas, reservoirs also emit methane (CH_4) which could negate some of the carbon benefits of switching to hydropower. CH_4 is a potent greenhouse gas with >32 times the warming potential of carbon dioxide over a 100-year time horizon (Etminan et al., 2016). Prior global CH_4 emissions estimates suggest 3 Tg C of CH_4 yr^{-1} is released from reservoir surfaces (Barros et al., 2011). This estimate increases to 13.3 Tg C as CH_4 yr^{-1} after accounting for spillways, turbines, river reaches below dams, and periodically inundated drawdown areas around the reservoir (Li & Zhang, 2014). While useful, these estimates are based on empirical relationships between emissions and potential drivers, and do not provide a process-based understanding of the main drivers and pathways for reservoir CH_4 production and releases, which would aid in development of mitigation strategies. Here we develop, evaluate, and apply a new mechanistic model of the processes driving global hydroelectric reservoir CH_4 emissions.

Methane production in hydropower reservoir occurs in sediments where anaerobic microbes respire carbon and produce CH_4. Methane is also thought to be produced in the oxic water column (Bižić et al., 2020; Bogard et al., 2014; Grossart et al., 2011; Günthel et al., 2019; Yao et al., 2016), though other studies conclude that sediment fluxes rather than oxic methanogenesis explain CH_4 concentrations in oxygenated surface waters (Peeters et al., 2019). Methanogenesis is fueled by carbon inputs for methanogenesis from primary production within the reservoir (Deemer et al., 2016; DelSontro et al., 2019), allochthonous carbon from the watershed (Jansson et al., 2007; Jones, 1992), and vegetation and soil carbon flooded during reservoir creation (Abril et al., 2005; Barros et al., 2011; Tremblay et al., 2005; Venkiteswaran et al., 2013). The initial carbon stocks in place during reservoir flooding can fuel an initial pulse in CH_4 production. Methane produced in hydroelectric reservoirs is released to the atmosphere via diffusion at the air-water interface, ebullition from the sediments, and vascular transport in emergent and floating-leaved aquatic plants (Bastviken et al., 2011; Borrel et al., 2011; Casper et al., 2000; Walter et al., 2006). CH_4 can also be emitted at turbine outlets (and immediately downstream of dams), where dissolved CH_4 in the water can quickly degas to the atmosphere (Fearnside, 2002; Kemenes et al., 2007). The GHGSat satellite instrument observed such a plume over the Lom Pangar dam in Cameroon (Jervis et al., 2021).

Understanding global CH_4 emissions from hydroelectric facilities is critical to evaluating the greenhouse gas contribution of this power source. Prior studies have identified correlations between reservoir CH_4 emissions and potential drivers as littoral area, mean annual temperature, age, chlorophyll *a* concentration, and mean depth (Barros et al., 2011; Deemer et al., 2016; DelSontro et al., 2019). Predictor variables such as total phosphorus, latitude, and temperature are inconsistent across studies, and some models neglect emissions from turbine degassing and downstream emissions, which can be comparable to emissions from ebullition (Deemer et al., 2016). More recently, the GHG Reservoir Tool (G-RES) has been developed to help reservoir managers estimate potential CH_4 emissions (Prairie et al., 2017). The G-RES tool includes a broad range of predictor variables for reservoir greenhouse gas emissions, but relies on empirical relationships that have limited predictive power beyond the range of available data.

The main objective of this study is improve understanding of the dominant drivers and pathways of methane emissions from hydropower reservoirs. We focus on several key questions: (a) Which carbon inputs dominate methane production? (b) What is the magnitude of global CH_4 emissions from hydropower and how is it distributed among individual reservoirs? And (c) What is the contribution from turbine degassing and under what conditions could it be seen from space? To answer these questions, we develop, evaluate, and apply a new semi-empirical model for CH_4 emissions to the atmosphere ((Res)ervoir (M)ethane (E)missions model, or ResME). ResME is based on best-available understanding of the biogeochemical processes contributing to CH_4 production and emission from hydropower reservoirs, evaluated using data from 54 reservoirs globally, and scaled-up to estimate global emissions. The model provides insight into the biogeochemical processes controlling hydropower CH_4 emissions. Results provide a new global, spatially resolved inventory of CH_4 emissions from hydroelectricity that can be used as prior estimate in inversions of atmospheric CH_4 observations. We use our analysis to identify key uncertainties in processes affecting global CH_4 from hydropower facilities and discuss data needed to improve future emissions projections.

2. Model Development

ResME includes parameterizations for (Figure 1):

1. Carbon inputs to methanogenesis from flooded soil and biomass carbon, autochthonous input, and allochthonous input
2. CH_4 production in anoxic sediment
3. CH_4 release via diffusion, ebullition, and vascular transport, and turbine degassing release.

2.1. Carbon Inputs to Methanogenesis From Autochthonous Input, Allochthonous Input, and Flooded Carbon

We include three sources of organic carbon (C_t in Equation 1) as substrate for methanogenesis: (a) autochthonous carbon generated by primary producers (such as algae) within the reservoir; (b) allochthonous carbon from inflowing rivers; and (c) the soil carbon and biomass carbon present in the reservoir landscape prior to flooding.

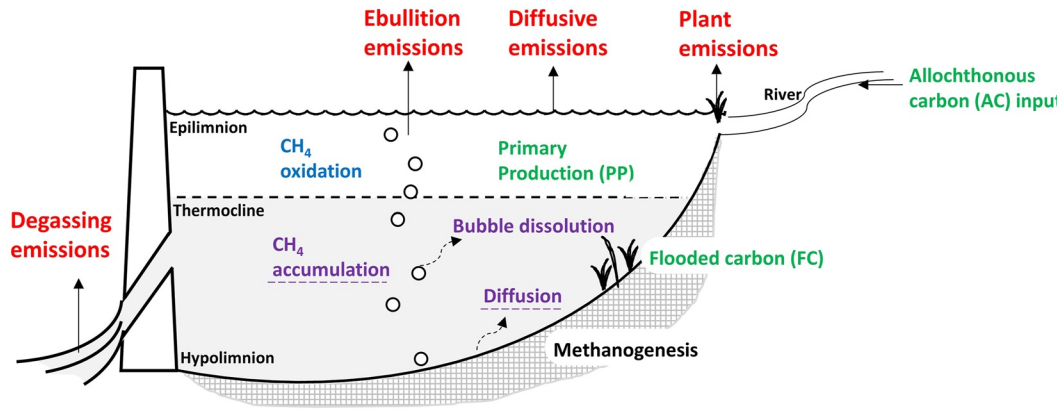

Figure 1. Schematic of hydroelectric reservoir and factors contributing to CH_4 production and transport. Carbon sources for methanogenesis are shown in green, CH_4 emissions pathways in red, CH_4 removal pathway in blue, and internal CH_4 fate/transport pathways in purple. Dashed arrows indicate internal transport. All sources and fates shown are explicitly modeled, except for those with dashed underlines (diffusion and CH_4 accumulation).

2.1.1. Autochthonous Input

We estimate autochthonous carbon (carbon coming from inside the aquatic system, in this case the reservoir) primary production in different reservoirs using literature-reported trophic status. Trophic status is a categorization reflecting the amount of biological productivity occurring in a water body. Trophic status is reported in the literature as oligotrophic (low productivity), mesotrophic (medium productivity), or eutrophic (high productivity). Each trophic state has a characteristic range of nutrient loading, chlorophyll *a* concentration, and primary productivity (such as algal growth) (Wetzel, 2001). Primary production in freshwater systems ranges from less than 50 mg C m^{-2} day^{-1} for oligotrophic systems to ~8,000 mg C m^{-2} day^{-1} for some highly eutrophic systems (Likens, 1975; Wetzel, 2001). We estimate mean primary production for oligotrophic, mesotrophic, and eutrophic reservoirs as 150, 600, and 2,000 mg C m^{-2} day^{-1}, respectively, following field measurements in Kimmel et al., 1990. Estimates of primary production in tropical reservoirs have higher uncertainty because data are only available for a few tropical systems. Not all autochthonous carbon settles to the sediment where it is available for methanogenesis. The ratio of autochthonous carbon that does settle is referred to as the "export ratio" and mean export rates across a range of studies are approximately 40 ± 20% (Baines & Pace, 1994; Berman et al., 2010; Darchambeau et al., 2005.; De Vicente et al., 2008; Ostrovsky & Yacobi, 2010; Steinsberger et al., 2021; Teodoru et al., 2013). Based on these studies, we use a constant export ratio of 40% across reservoirs.

2.1.2. Allochthonous Input

Allochthonous carbon is carbon sourced from outside the aquatic system, such as from the surrounding watershed. Dissolved and suspended particulate organic carbon (DOC and POC, respectively) is delivered to reservoirs by rivers, and a portion of each carbon form is subsequently buried in the sediment (Wachenfeldt et al., 2009). We estimate POC inputs to sediment based on the total river sediment load (Equation S1–S3 in Supporting Information S1; Meybeck, 1982). Total sediment load estimates are estimated using the WBMsed model (Cohen et al., 2013), which calculates monthly estimates of sediment load at 0.1° spatial resolution. We used annual average sediment loading from 2001 to 2019, and for each reservoir location we assumed sediment concentration was equivalent to the flow-weighted mean for the 1° box centered on the reservoir coordinates. Allochthonous POC input is then estimated as a function of total sediment load (Meybeck, 1982, see details in Supporting Information S1). Since not all sediment entering the reservoir will be trapped, we estimate trapping efficiency based on hydraulic residence time (Equation S1 in Supporting Information S1, Vörösmarty et al., 2003). The ratio of DOC to total organic carbon (DOC + POC) has been found to decrease with increased suspended sediment load (Meybeck, 1982, see details in Supporting Information). Flocculation (aggregation of fine particles and settling) rates for incoming DOC vary with temperature (Equation S2 in Supporting Information S1, Wachenfeldt et al., 2009).

2.1.3. Flooded Carbon

Annual average organic carbon for 12 different carbon pools (including leaf, fine root, wood, and woody debris pools, as well as metabolic, structural, and both above- and below-ground microbial pools) within each flooded reservoir is estimated as the carbon content in the corresponding grid cell as modeled by a global terrestrial carbon model with 0.5° × 0.5° gridded monthly resolution (SibCASA, Huntzinger et al., 2018; Schaefer et al., 2008). Flooded carbon input at the time of reservoir creation was assumed to be the sum of the SibCASA carbon pools at the reservoir location. Since lignin inhibits decay (Van Coillie et al., 1983) to the point that no wood decay was observed in a recently flooded reservoir (Hall & St Louis, 2004), we excluded the SibCASA carbon pools of wood and woody debris.

2.2. Methane Production in Anoxic Sediment

We model monthly CH_4 production (P_t, mg CH_4 m^{-2} day^{-1}) associated with decay of organic carbon following (Vachon et al., 2017):

$$P_t = \frac{dC}{dt} = \eta \times \underline{k_t} \times C_t \quad (1)$$

where C_t is the bulk carbon content of age t in the sediment (mg C m^{-2}), $\underline{k_t}$ is the age-dependent decay constant for the mixture of organic material, and η reflects the fact that some carbon is converted to CO_2 instead of CH_4. The exact ratio of carbon conversion depends on the fraction of aerobic to anaerobic decomposition and the ratio of acetoclastic to hydrogenotrophic methanogenesis (Conrad, 2005). ResME determines this empirically by minimizing the fractional bias between model results and field measurements. Since Equation 1 represents the methanogenesis for carbon of a particular age, carbon pools containing carbon of different ages will require a sum of P_t values (see Equation 3).

2.2.1. Reactive Continuum Model for Organic Carbon Decay (k)

Recent work has shown that reactive continuum decay models successfully predict decay patterns for heterogeneous carbon pools (Catalan et al., 2017; Koehler & Tranvik, 2015). Reactive continuum models allow the decay rate to vary based on organic carbon type, and to change during the decomposition process as labile compounds are consumed (Boudreau & Ruddick, 1991; Koehler et al., 2012; Mostovaya et al., 2017; Vachon et al., 2017). Variable decay rates are important because biomass from autochthonous primary production is more readily degraded by methanogens compared to other terrestrial carbon sources (Gudasz et al., 2012; West et al., 2016; Zhou et al., 2019). Additionally, non-lignin components of biomass are more labile than wood, which is relatively recalcitrant (Koehler & Tranvik, 2015; Moran et al., 1989).

We used the reactive continuum decay model to estimate the apparent decay constant, k, following the parameterization described by (Boudreau et al., 2008), and the Arrhenius correction for temperature described by (Venkiteswaran et al., 2007):

$$\underline{k} = \frac{v}{(a + t)} \times 1.047^{(T-20)} \quad (2)$$

where t is carbon age (in months), α is a rate parameter related to the average lifetime of the more labile carbon compounds, v is a unitless parameter related to the relative abundance of more recalcitrant compounds (Boudreau et al., 2008), and T is sediment temperature (°C). Where reactive continuum modeling has typically been done on a daily scale, we applied the method on a monthly scale to reduce computation time.

We extracted monthly reactive continuum decay parameters for autochthonous carbon (phytoplankton) and allochthonous carbon (terrestrial leaf) decay from a study on organic matter decomposition in anoxic freshwater sediment (Grasset et al., 2018). Grasset et al., 2018 provide data on carbon decomposition over time, which we fit to the reactive continuum model:

$$\frac{\text{Mass}_{t=t}}{\text{Mass}_{t=0}} = \left(\frac{\alpha}{\alpha + t}\right)^{v} \quad (3)$$

Table 1
Decay Constants Used in Reactive Continuum Decay Modeling for Autochthonous, Allochthonous, and Flooded Carbon Sources

	α[a] (months)	v[b] (dimensionless)
Autochthonous carbon	0.61	0.46
Allochthonous carbon	0.15	0.917
Flooded carbon	0.15	0.917

Note. All parameters are derived from data in Grasset et al. (2018).
[a]Average lifetime of the more reactive compounds. [b]Relative abundance of the most recalcitrant compounds.

where α and v are the decay parameters, t is time in months, $\text{Mass}_{t=0}$ is the initial carbon mass and $\text{Mass}_{t=t}$ is the carbon mass at month t. We ran a least squares regression with the scipy package in Python Version 3.7.4 to select the optimal α and v decay parameters for flooded carbon, which are provided in Table 1. We assume that flooded biomass carbon will behave similarly to the terrestrial leaf. Section 4.0 discusses ResME sensitivity to decay parameters.

Allochthonous and autochthonous carbon are continually being added to a reservoir system. Upon addition to the model reservoir, a portion of this 0-month-old carbon is mineralized (following Equations 1 and 2, where $t = 0$) and the remainder rolls over into the 1-month-old carbon pool where t becomes 1 (Figure 2). The modeling therefore requires accounting for the monthly input of fresh carbon, the transfer of unmineralized carbon after each month to the next oldest age pool, and different decay parameters for every age pool. After accounting for these additions, the total CH_4 production (P_{tot}) for a reservoir of age N is:

$$P_{tot} = \sum_{C\text{source}} \sum_{t=0}^{N} \eta \times \frac{v}{\alpha + t} \times C_t \times 1.047^{(T-20)} \quad (4)$$

where t is the age of the carbon input in each monthly age class, η is a fitted parameter to minimize fractional bias between model results and field measurements, N is the current age of the reservoir, T is the sediment temperature, C_t is the carbon content in each monthly age class, and results from different carbon sources (C_{source}) are summed.

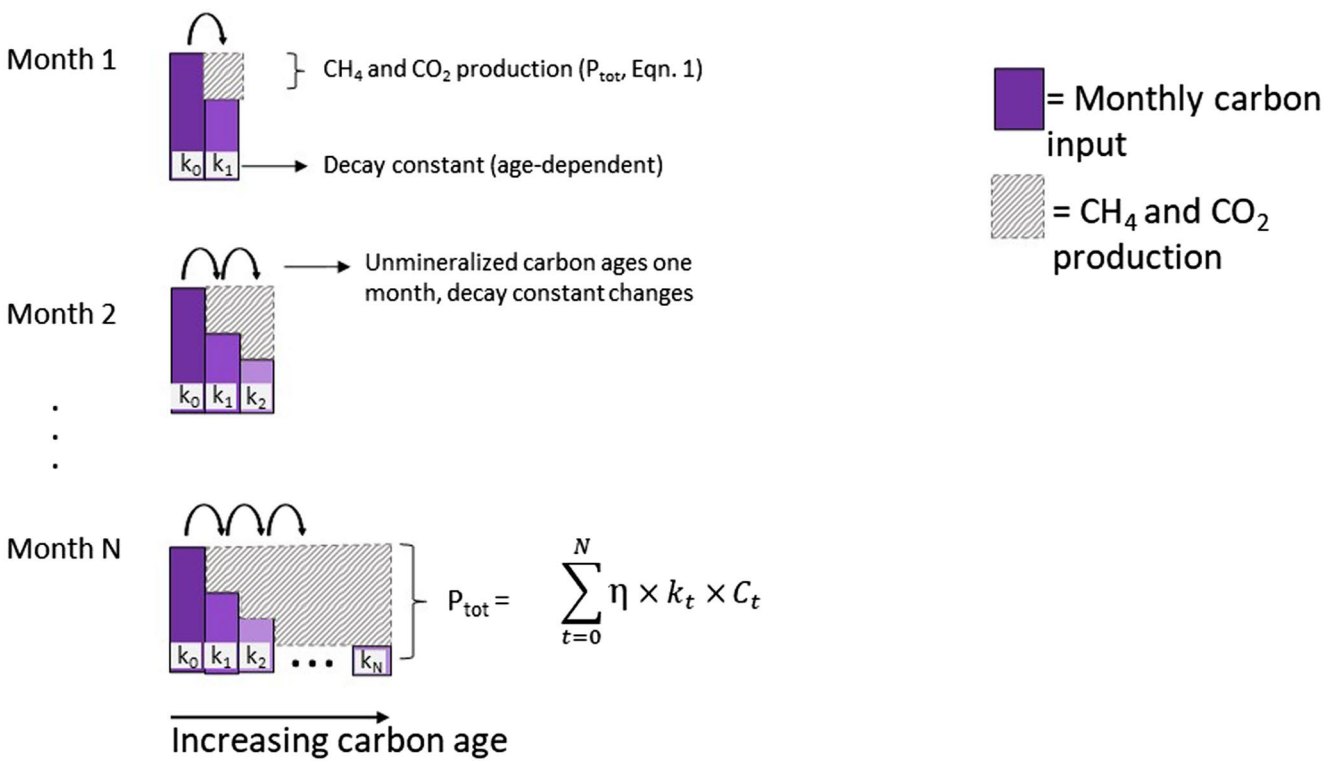

Figure 2. Model schematic showing carbon pool progression across lifetime of reservoir (age = N), for one carbon type. Total methanogenesis (P_{tot}) is the sum of methanogenesis from each carbon type (autochthonous, allochthonous, and flooded carbon). Variable descriptions are associated with Equations 1 and 2 in the main text.

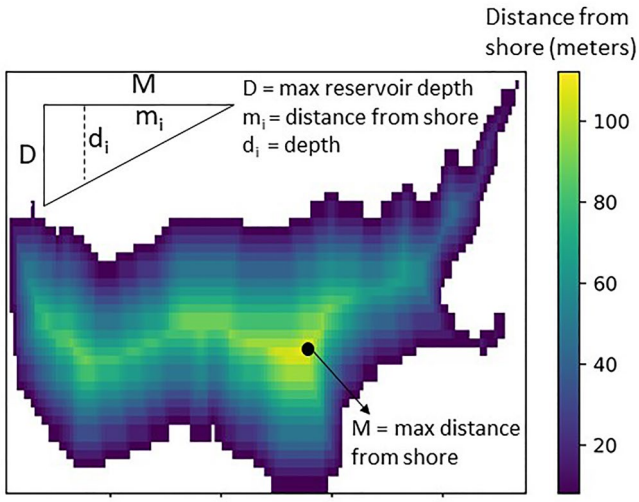

Figure 3. Estimated bathymetry for Foster reservoir in Oregon, USA based on the reservoir footprint and maximum depth.

2.2.2. Sediment Temperature

Sediment temperature affects methanogenesis rates and total CH_4 production. Sediment temperature is affected by reservoir stratification status (i.e., sediment in deeper, unmixed waters is colder than in littoral, well mixed waters). Lake water temperatures can be modeled using the one-dimension thermodynamic model, FLake (Mironov et al., 2010). FLake results per grid cell are included into the global modeling output from European Center for Medium-Range Weather Forecasts (ECMWF) reanalysis product, known as ERA5 (C3S: Copernicus Climate Change Service, 2017). In the absence of reservoir-specific models for water temperature, we assume that FLake results are reasonable for reservoirs, and extracted FLake model results using Google Earth Engine (Gorelick et al., 2017) for reservoir bottom layer temperature, mixed layer temperature, and mixed layer depth. We computed monthly average temperatures and mixed layer depth from 2015 to 2021.

To translate the epilimnetic temperatures and hypolimnetic temperatures to an areal basis, we needed to estimate the fraction of each reservoir with sediments above and below the mixed layer depth. While we do not have detailed bathymetry for each reservoir in the set of reservoirs with field CH_4 estimates that we use for model comparison, the Global Reservoir and Dam Database (GRanD) database provides footprints for many reservoirs (Lehner et al., 2011). We simulated the bathymetry of each reservoir by assuming a linear slope between reservoir shore and the maximum basin depth at the maximum distance from shore (Figure 3). The resulting sediment slope provides an estimated water column depth throughout the reservoir (see Figure 3 inset). For all reservoirs, dam heights are available from GRanD or individual sources (see Table S2 in Supporting Information S1). We estimate the maximum reservoir depth as 90% of the dam height, thereby roughly accounting for the vertical distance between the designed water surface and the top of the channel bank (freeboard). We use this modeled bathymetry to estimate the sediment surface area at depths greater and less than the mixed layer depth provided in the ERA5 output. For reservoirs in our comparison data set that do not have GIS footprints in GRanD, use the estimate of littoral area ratio used in the G-Res model (Prairie et al., 2017).

2.3. Methane Release via Diffusion, Ebullition, and Vascular Transport, and Turbine Degassing Release Assuming Deep Water Turbine Intake

The fate of CH_4 produced in the reservoir sediment (P_{tot}, mg C/m^2/day, Equation 5) is partitioned by mass balance in to five potential fates:

$$P = Ox + E_b + D_f + T_b + A_p \quad (5)$$

where Ox is internal oxidation, E_b is ebullition, D_f is diffusive emission, T_b is emission through turbines (or immediately downstream of the dam), and A_p is transport through plant tissue (parameter estimates explained below). Oxidation is the only fate that reduces the total amount of CH_4 available for partitioning between the four potential emission pathways. The balance of CH_4 partitioning between oxidation, diffusion, ebullition, turbine output, and plant tissue is determined by complex interactions between physical, chemical, and biological forces across both space and time. ResME uses simple theoretical relationships and literature estimates to parameterize and estimate the five potential CH_4 fates.

2.3.1. Oxidation and Downstream Emissions

Internal oxidation within a stratified reservoir is thought to occur primarily along the oxycline, where CH_4 diffuses upwards and encounters aerobic methanotrophs in oxygenated water or sediment. Methane is rapidly depleted at the oxycline, and the amount of CH_4 diffusing upwards determines the rate of oxidation. Processes that decrease the amount of dissolved CH_4 in the hypolimnion of the reservoir will decrease internal CH_4 oxidation at the oxycline. Thus, turbines that pull water from a CH_4-rich hypolimnion will directly reduce the amount of CH_4 available for oxidation. Turbines that pull water from a CH_4-poor epilimnion should not affect oxidation rates. ResME therefore assumes Ox and T_b are directly and negatively coupled such that increased CH_4 release

through the turbines leads to a decrease in internal oxidation within reservoirs. ResME does not include emissions estimates for turnover events, when potentially CH_4-rich water from the hypolimnion gets mixed with the epilimnion and can diffuse to the atmosphere. Some studies suggest that CH_4 oxidation during turnover is rapid enough to prevent significant CH_4 emissions (Kankaala et al., 2007; Mayr et al., 2020; Schubert et al., 2012.; Utsumi et al., 1998), though this is not true for all water bodies (Fernández et al., 2014).

Much of the literature on whole-system oxidation rates (Ox) comes from relatively shallow lakes, where oxidation is typically found to consume roughly 50%–90% of total CH_4 production in shallow lakes (Bastviken et al., 2008; Kankaala et al., 2006; Matthews et al., 2005; Rudd & Hamilton, 1978; Schmid et al., 2017). This estimate for oxidation as a percent age of production in shallow lakes can be expanded to deeper water bodies by considering that in deep water, bubble dissolution can contribute significantly to the amount of dissolved CH_4 available for oxidation or diffusive emission to atmosphere (Delwiche & Hemond, 2017; Schmid et al., 2017). The amount of bubble dissolution is a function of reservoir depth (McGinnis et al., 2006). We therefore assume that total potential oxidation (Ox) is a minimum of 80% (future additions to ResME could vary this estimate based on reservoir characteristics) of total CH_4 production, plus a depth-dependent fraction to account for bubble dissolution:

$$Ox + T_b = (0.8 + \mathrm{Bub_{diss}}) \times P \tag{6}$$

where $\mathrm{Bub_{diss}}$ describes a linear increase in oxidation and/or turbine release with reservoir depth (described below). Thus, we estimate that when turbines pull from the hypolimnion, maximum potential turbine release is $(0.8 + \mathrm{Bub_{diss}}) \times P$, and internal oxidation is zero. This assumption provides a theoretical upper ceiling on potential methane release, because in reality some internal CH_4 oxidation will occur as dissolved CH_4 diffuses upwards through the oxycline. Conversely, turbine release is assumed to be zero when turbines pull from the epilimnion, and internal oxidation is $(0.8 + \mathrm{Bub_{diss}}) \times P$.

To estimate $\mathrm{Bub_{diss}}$, we first recognize that typical bubble diameters in aquatic systems are 4–6 mm upon release from sediment (though there is large variation) (DelSontro et al., 2015; Delwiche & Hemond, 2017; Ostrovsky et al., 2008), and 4–6 mm bubbles are expected to completely dissolve after rising through approximately 60m of water (McGinnis et al., 2006). We therefore model the spatially average $\mathrm{Bub_{diss}}$ as:

$$\mathrm{Bub_{diss}} = \begin{cases} 0.15 \times \dfrac{d}{60} & \text{for } d < 60\,\mathrm{m} \\ 0.15 & \text{for } d \geq 60\,\mathrm{m} \end{cases} \tag{7}$$

where d is the average reservoir depth (m). The 0.15 parameter represents the maximum fraction of CH_4 production that could contribute to bubble dissolution. This parameter is less than 0.2 because even in deep systems, some of the produced CH_4 will still escape to the atmosphere from littoral zones. We note that ResME does not directly estimate the amount of methane released from the sediment via ebullition, and therefore cannot partition bubble dissolution and bubble emission (unlike G-Res, which does partition ebullition and diffusion using empirical relationships, Harrison et al., 2021). Partitioning ebullition and diffusion has been done in more complex models focused on methane emissions from boreal and arctic reservoirs (Stepanenko et al., 2011; Tan et al., 2015), but partitioning requires additional information about sediment porosity and atmospheric pressure which would confound the goal of building ResME for mechanistic, global-scale reservoir methane emissions estimates. The need to estimate bubble dissolution arises because studies in shallow lakes indicate that roughly 80% of methane is oxidized, but total oxidization is expected to be higher in deeper systems in part because a higher percentage of methane from bubbles will dissolve and be subject to oxidation.

To accurately estimate total annual degassing through turbines, we would need a monthly assessment of reservoir stratification. The occurrence and duration of stratification is a function of parameters such as water transparency, wind speed, and reservoir morphology, and can be modeled with significant input data (Lee et al., 2013; Noori et al., 2019; Yigzaw et al., 2019). Since individual reservoir modeling for stratification is beyond the scope of ResME, we instead provide degassing estimates for two potential scenarios: (a) maximum possible degassing if reservoirs were stratified year-round and thus $T_b = (0.5 + \mathrm{Bub_{diss}})\ x\ P$ in each month, and (b) reservoir is stratified for the 2 months before and after peak reservoir temperature (5 months total), with monthly degassing zero otherwise. These scenarios provide an upper limit and reasonable assessment for annual degassing estimates, with more accurate estimates requiring more detailed knowledge of monthly stratification status. We note that the

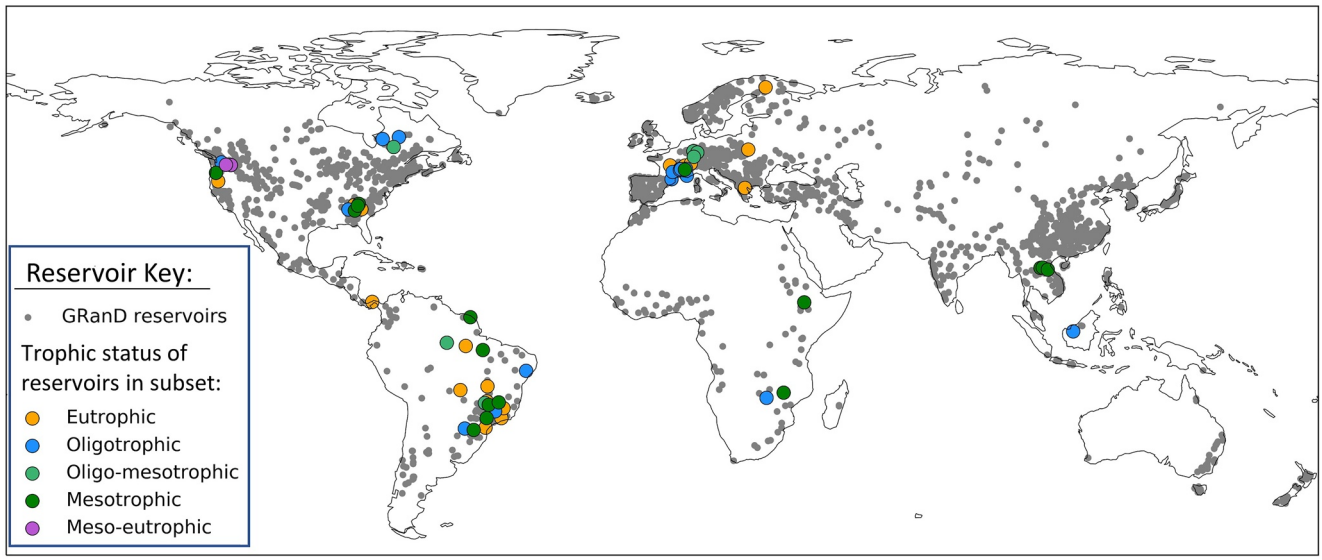

Figure 4. All hydroelectric reservoirs in the Global Reservoir and Dam Database database (gray dots). Reservoirs with field data that were compared to model results ("reservoir subset") are color-coded according to trophic status.

ISIMIP lake sector provides stratification estimates for generalized reservoirs on a 0.5° × 0.5° global grid (Golub et al., 2022), and may be useful in future updates to ResME.

2.3.2. Plant Emissions

Total transport through vascular plant tissue (A_p) depends on many factors, including plant type, water column depth, plant coverage, and length of vegetation period. Bastviken et al. (2011) estimate vascular plant transport (A_p) at approximately 16% of emissions due to diffusion and ebullition ($E_b + D_f$), which is a rough estimate given the complexity governing plant transport, and the likelihood that reservoirs experiencing large water-level fluctuations have fewer emergent macrophytes:

$$A_p = 0.16 \times (E_b + D_f) \tag{8}$$

2.3.3. Diffusive and Ebullitive Emissions

Combining Equations 5–8 yields an estimate of ebullitive and diffusive emissions that depends on total CH_4 production (P_{tot}) and the depth-dependent parameter Bub_{diss}:

$$E_b + D_f = \frac{P}{1.16}[1 - (0.8 + Bub_{diss})] \tag{9}$$

Many field studies report ebullition and diffusion estimates from reservoir surfaces, and we can compare these field estimates with the estimations from Equation 9.

3. Evaluating Model Results

3.1. Field Measurements for Comparison

Diffusive and ebullitive CH_4 measurements, and all necessary ancillary information for ResME were available for 54 hydroelectric reservoirs (hereafter referred to as the "reservoir subset"). Many of these studies were compiled by Barros et al., 2011, Deemer et al., 2016, and Prairie et al., 2017, with a few more having been published more recently (Table S2 in Supporting Information S1). These reservoirs represent a range of sizes, flow rates, and geographical locations spanning the globe (Figure 4). We can compare these reservoirs to the 2,462 hydropower reservoirs in GRanD, where GRanD is a global, geographically referenced list of reservoirs and associated metadata (Lehner et al., 2011). The reservoir subset over-represents large reservoirs compared to their size-based prevalence in GRanD, while flow rates and latitude are more representative of GRanD values (Figure S1 in

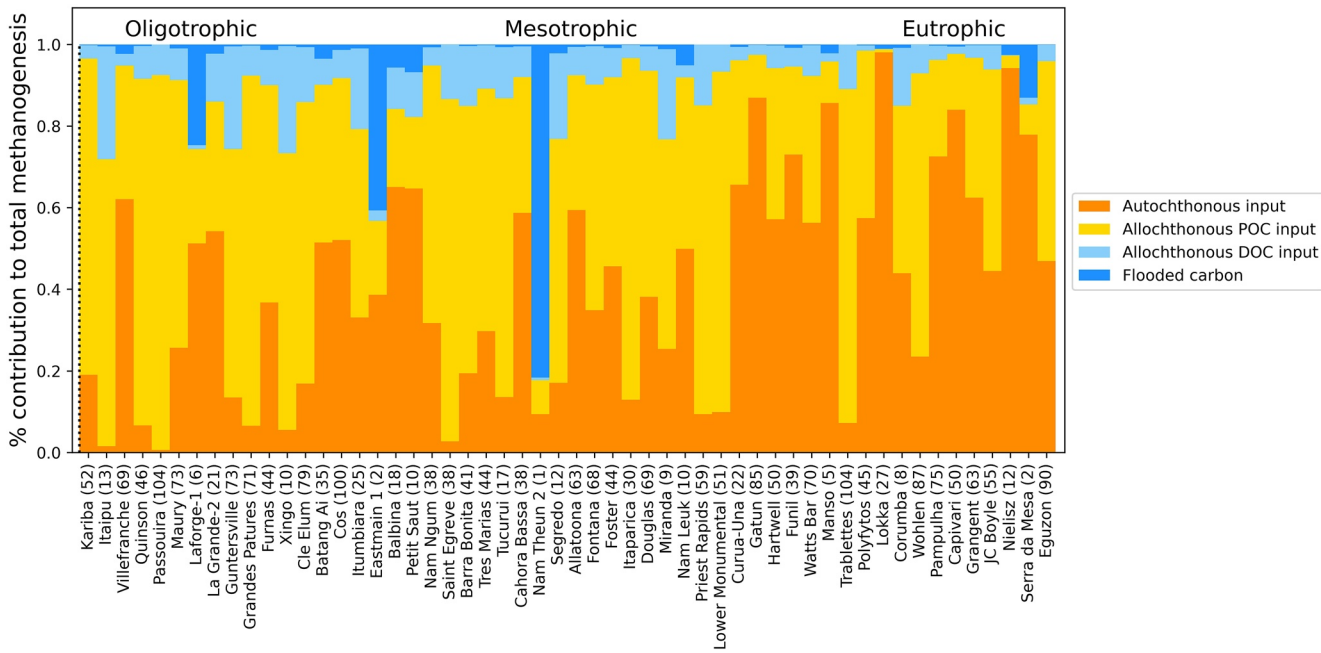

Figure 5. Carbon source for daily methane (CH_4) production, shown as percentage of total methanogenesis, and colored by carbon type. Reservoirs are grouped by trophic status, and parenthetical numbers after reservoir names are reservoir ages, in years.

Supporting Information S1). The 54 reservoirs in our subset represent 12% of the discharge from all reservoirs in the GRanD database, which reflects the fact that the observational data are skewed toward large systems. Reservoirs in the subset contain a relatively even mix of trophic statuses (18 oligotrophic to oligo-mesotrophic reservoirs, 16 mesotrophic reservoirs, and 20 meso-eutrophic to eutrophic reservoirs). Average reservoir age is 44 years, which means most reservoirs will be beyond the initial pulse of methane production reported for most systems shortly after reservoir creation.

3.2. Contribution of Each Carbon Source to Methanogenesis

For most of the reservoir subset, ResME estimates that the majority of methanogenesis comes from the decay of autochthonous carbon and allochthonous POC inputs (40 ± 27% and 47 ± 25% of total methanogenesis, respectively), with allochthonous DOC contributing another 8 ± 7%. Allochthonous POC tends to be more important for oligotrophic and mesotrophic systems, whereas autochthonous carbon is the primary carbon source for methanogenesis in many of the eutrophic reservoirs. The relative contribution of flooded biomass to total methanogenesis is highly dependent on reservoir age. Since the average age of reservoirs within our subset is 44 years, and peak methane production from flooded biomass occurs within a decade of reservoir creation, the CH_4 contribution from flooded biomass is low (4 ± 12% of total methanogenesis). Relative contributions from flooded carbon to methanogenesis will be much higher in very young systems; for example, reservoirs less than 7 years old had more than 20% of their methanogesis come from flooded carbon (Figure 5). While the relative contributions from different carbon sources are useful for understanding the dominant drivers of methanogenesis in reservoirs, the uncertainty associated with these estimations is high (see Section 4.2, Uncertainty).

3.3. Ebullitive and Diffusive Emissions

ResME predictions for ebullitive and diffusive CH_4 emissions correlate well with field measurements ($r^2 = 0.41$, $p = 0.0001$, mean fractional bias = 0.01 in log space) with $\eta = 0.35$. We fit η to minimize the mean fractional bias between ResME estimates and field observations, where mean fractional bias is:

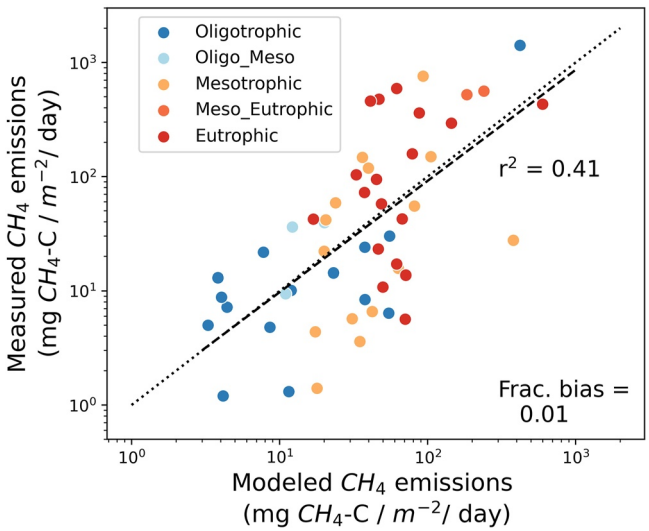

Figure 6. Comparing field measurements of methane (CH_4) flux to model output. Dashed black line is the linear regression fit in log-log space, and dotted black lines represent a 1:1 relationship between measured and modeled CH_4 emissions. Markers are color-coded by reservoir trophic status.

$$\text{MFB} = \frac{2}{N}\sum_{i=1}^{N}\frac{C_{m,i} - C_{o,i}}{C_{m,i} + C_{o,i}}$$

where C_m and C_o are the model-predicted and observed ebullition plus diffusion flux (respectively), and N is the number of reservoirs (Boylan & Russell, 2006; Zhang et al., 2014). As expected, model results are typically highest for eutrophic systems and lowest for oligotrophic systems (Figure 6). The fitted η value of 0.35 indicates that on average 35% of the respired carbon is available for methanogenesis, while 65% becomes CO_2.

3.4. Downstream Emissions

Methane emission estimates for maximum potential turbine degassing can be compared to field campaigns measuring degassing at reservoirs where turbine water intake is well below a stratified thermocline (the theoretical maximum degassing calculated by ResME occurs from deep turbine intakes). We found four previously studied reservoirs with annual degassing estimates from deep-water intakes. As described earlier, we estimate maximum potential annual emissions if reservoirs were permanently stratified, and emissions assuming 5 months of stratification during the warmest months (Table 2). Of the reservoirs with degassing estimates, Tucurui, Balbina, and Batang Ai are all reported to stratify year-round (Fearnside, 2002; Kemenes et al., 2007; Soued & Prairie, 2020), whereas Petit Saut has periods of mixing throughout the year (Abril et al., 2005). ResME estimates of turbine degassing assuming annual stratification are on average 180% of measurement estimates.

ResME estimates of turbine degassing could be higher than observed measurements because methane oxidation occurs during degassing and downstream from the turbines, but this is not accounted for in the model. For example, approximately 8%, 10%, and 40% of the CH_4 released through turbines is estimated to be oxidized downstream of the Petit-Saut dam, Batang Ai dam and Balbina dam, respectively (Fearnside, 2002; Kemenes et al., 2007; Soued & Prairie, 2020). Thus for the global upscaled estimate of potential turbine degassing, we assume that 20% of the released methane is oxidized prior to release to the atmosphere. While ResME provides a reasonable order-of-magnitude estimate of CH_4 turbine degassing, accurately upscaling estimates of turbine CH_4 outputs would require information about turbine intake height at each reservoir, as well as seasonal stratification patterns. Field measurements for systems that pull water from the epilimnion are dramatically lower than those systems which draw water from the hypolimnion, since the epilimnion waters are often much lower in dissolved CH_4 (Chanudet et al., 2011).

Table 2
Field Estimates of CH_4 Dam Degassing Compared With ResME Maximum Potential Degassing Estimate (Gg CH_4-C/yr)

System	Annual degassing estimates from field measurements (Gg CH_4-C/yr)	Maximum potential degassing estimate from ResME (Gg CH_4-C/yr)	
Stratification assumption		Permanently stratified	5-month stratification[a]
Tucurui	527 (Fearnside, 2002)	664	285
Balbina	65 (Kemenes et al., 2007)	61	27
Petit Saut	7.5 (Abril et al., 2005)	20	9
Batang Ai	0.55 (Soued & Prairie, 2020)	1	0.5

Note. These four reservoirs stratify in the summer and have turbine intakes below the thermocline.
[a]Assuming the 5 months include the month of maximum methane production, plus the 2 months before and after the maximum month.

3.5. Using Autochthonous Carbon as Proxy for Methane Production

Previous studies have found chlorophyll *a* concentrations to be correlated with CH_4 emissionsCH_4 emissions (estimated by chlorophyll *a* concentration: Deemer et al., 2016; DelSontro et al., 2019, Deemer & Holgerson, 2021). Chlorophyll *a* can be seen as a proxy for autochthonous carbon, and ResME results when only including autochthonous carbon generate reasonable fits between measurements and model for reservoirs with longer water residence time (Figure S6 in Supporting Information S1). However, CH_4 emissions from some run-of-river reservoirs with short water residence times are not well described with only autochthonous carbon. This could indicate that allochthonous carbon plays a larger role in reservoir CH_4 emissions for reservoirs with short residence times, compared to reservoirs with long residence times. This hypothesis is supported by studies showing that the ratio of

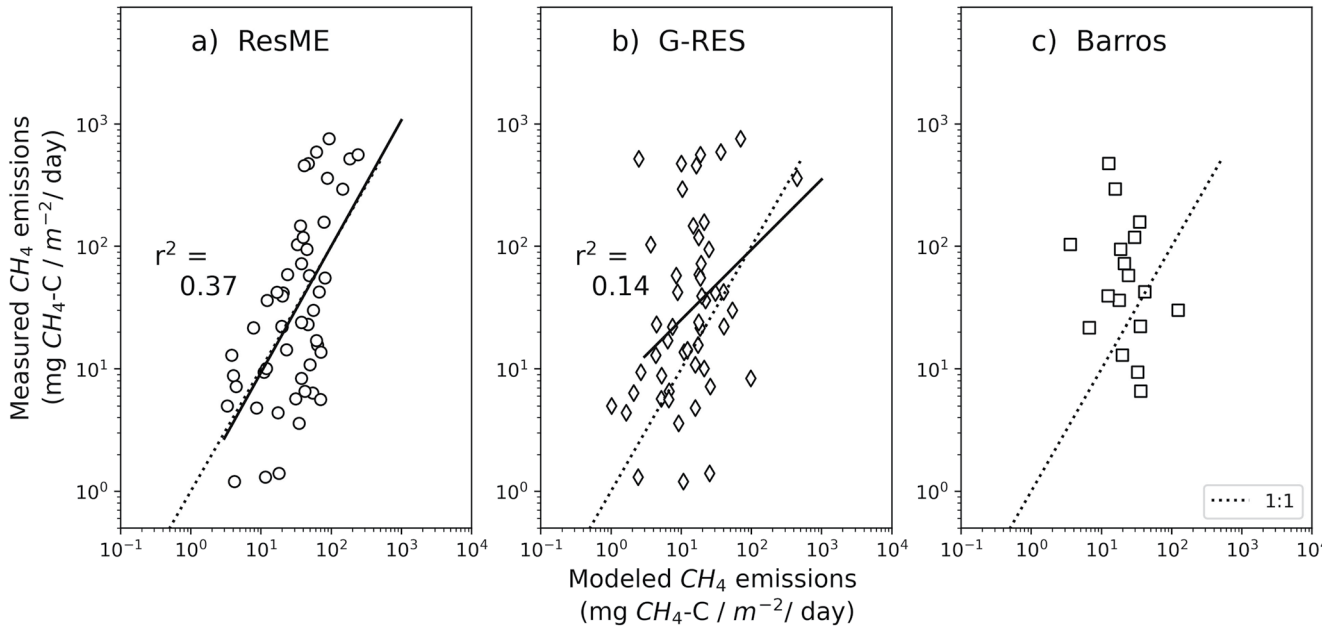

Figure 7. Comparing model performance against field data for (a) (Res)ervoir (M)ethane (E)missions (ResME) (this study), (b) the G-RES model (Prairie et al., 2017) and (c) the model described by Barros et al., 2011. Model fits with measured emissions, along with r^2 values, are shown for ResME and G-RES. Model fit for Barros estimates had to be tested again a smaller subset of reservoirs since not all reservoirs had dissolved organic carbon measurements. Model fit for Barros data were not significant, while the ResME fit for the same set of reservoirs was significant ($p < 0.05$, $r^2 = 0.39$). Black dotted line represents 1:1.

allochthonous to autochthonous carbon is higher in reservoirs with shorter residence times (Hanson et al., 2015; Park et al., 2009).

3.6. Comparisons With Existing Methods to Estimate CH_4 From Hydropower

The G-res tool, described in Prairie et al., 2017, provides empirical methods to estimate greenhouse gas emissions (including CH_4) from reservoirs, and includes estimations of emissions prior to, and during, reservoir construction. G-res estimates methane release from reservoir surfaces as a function of reservoir age, mean depth, maximum depth, incoming radiation, and temperature. We ran G-res and ResME for the same subset of reservoirs (Figures 7a and 7b). For G-res, we assumed the maximum reservoir depth was 5 m lower than the dam height (dam heights provided in GRanD). Both models have significant fits between modeled and measured emissions estimates, though the ResME fit has a higher r^2 value then G-res. Reported r^2 for comparisons between G-res CH_4 diffusion and ebullition model predictions and measurements were 0.52 and 0.26, respectively (Prairie et al., 2021). However, the r^2 for a comparison between G-res predicted diffusive-plus-ebullitive CH_4 emissions for the subset of reservoirs used to test ResME, was somewhat lower ($r^2 = 0.14$) than the values reported for the individual G-res submodels, and lower than that calculated here for ResME. We also include a comparison with the estimation method in Barros et al., 2011, where reservoir emissions were found to depend on reservoir age, mean depth, DOC concentration, and latitude. Using the Barros method, we estimated CH_4 emissions for the subset of reservoirs that contained DOC concentration measurements (Figure 7c). However, the Barros et al. method did not produce a statistically significant regression between modeled and measured emissions estimates ($p > 0.05$). These model comparisons demonstrate that ResME's focus on biogeochemical processes allow improved predictions of CH_4 emissions. A useful future improvement for ResME would be incorporating a process-based estimate of the percentage of incoming carbon available for methanogenesis.

The relatively high RMSE values for both ResME and G-res demonstrate that substantial uncertainty remains in understanding the drivers of methane emissions from reservoirs (where RMSE values on the log-log scape are 1.29 and 1.77 for ResME and G-res, respectively). Uncertainty is high both for the drivers of methane emissions, and for the field measurements. We discuss this further in the Uncertainty section below.

3.7. Other Measurements of Model Performance

3.7.1. Organic Carbon Sediment Storage

In addition to estimating CH_4 emissions from reservoir surfaces and dams, we also compare ResME estimates for organic carbon sediment storage rates to field measurements as a check on model performance. We estimate organic carbon storage for each carbon type (B_i) as:

$$B_i = C_i - P_{CH_4} - P_{CO_2} = C_i - \left[1 + \frac{1-\eta}{\eta}\right] P_{CH_4}$$

where C_i is the annual input of each carbon type, P_i is the estimated methanogenesis from that carbon source, and the factor of η accounts for the fraction of organic carbon converted to CH_4 compared with CO_2 (η is fitted to be 0.35). Given the uncertainties in input parameters, ResME estimates of B_i are approximate, yet are still useful as an order-of-magnitude check on whether ResME predictions match field measurements. The median ResME-estimated organic carbon sediment storage, was 328 gC m^{-2} yr^{-1}. This estimate is close to the median estimate of 279 gC m^{-2} yr^{-1} in a global compilation of field measurements from Mendonça et al., 2017 (Figure S5 in Supporting Information S1), even though Mendonça et al., 2017 used a different set of reservoirs. The general agreement between measured and ResME-modeled storage estimates is another indication that ResME results reflect field conditions reasonably well.

3.7.2. Temperature Results

ERA5 maximum surface water temperatures approximately match measured peak water temperatures across a wide range of latitudes (Figure S2a in Supporting Information S1), with some slight under-predicting in tropical regions that may be attributable to the fact that tropical reservoirs have historically been under-studied compared to higher-latitude systems (Winton et al., 2019). Hypolimnetic temperatures from ERA5 were consistent with measured temperatures (Figure S2b in Supporting Information S1). These comparisons indicate that ERA5 temperature estimates are reasonable for our reservoir subset.

3.7.3. Allochthonous Carbon Inputs

To assess the representativeness of the allochthonous POC inputs calculated in ResME, we compared ResME estimates of riverine total suspended solids (TSS) and POC concentration to global compilations of river measurements from the GEMS-GLORI database (Meybeck & Ragu, 2012) (Figure S3 in Supporting Information S1). The ResME distribution of TSS concentrations in our reservoir subset is significantly lower than the global distribution in GEMS-GLORI ($p < 0.005$, using a Kolmogorov-Smirnov test). Global mean and median TSS values are 1918 and 194 mg/L, respectively, while mean and median TSS from the ResME reservoir subset are 272 and 141 mg/L, respectively. Similarly, estimates for riverine POC are also higher than the global distribution from GEMS-GLORI ($p < 0.001$), with mean[median] of 8.9[2] mg/L globally, and 4.37[3.98] mg/L for the reservoir subset (Figure S4 in Supporting Information S1). This could be because ResME overestimates riverine POC inputs, because our reservoir test set is systematically biased toward rivers with higher POC concentrations, or potentially because GEMS-GLORI is biased. We discuss this further below.

4. Sensitivity and Uncertainty

4.1. Sensitivity Analysis

We conducted a sensitivity analysis to assess the relative importance of ResME assumptions about carbon input, methanogenesis, and CH_4 fate and transport. We individually increased input parameters by 5% and recorded the mean change in predicted CH_4 release across the 54 reservoir subset (Table 3). Our results show that for the set of assumptions governing carbon input to reservoirs, ResME is most sensitive to changes in the dominant carbon source. Increasing autochthonous, allochthonous DOC, or allochthonous POC carbon inputs by 5% raises mean modeled results by 2.0%, 0.4%, and 2.3%, respectively. We note that variations in reservoir age, particularly during the first decade after reservoir construction, may produce large changes in annual methane emissions.

Of the parameters affecting methanogenesis rates, ResME is most sensitive to changing the v decay parameter, then to changing sediment temperatures, and lastly to changing α parameters for autochthonous and allochthonous carbon. A 5% increase in the v decay parameter for autochthonous carbon and allochthonous carbon yields a

Table 3
Sensitivity Analysis

Treatment	Parameter or input	Mean change in predicted CH_4 release (%)	
Factors affecting carbon input			
+ 5%	Q (average reservoir discharge)		0.9
+ 5%	Fraction of POC in total sediment load		2.8
+ 5%	Flocculation rate		0.4
+ 5%	Autochthonous input		2.0
+ 5%	Flooded carbon input		0.2
+ 5%	Allochthonous POC input		2.3
+ 5%	Allochthonous DOC input		0.4
Factors affecting methanogenesis			
+ 5%	Epilimnion temperature		0.9
+ 5%	Hypolimnion temperature		1.3
+ 5%	Fraction of epilimnion area		0.1
+ 5%	Flooded carbon v decay parameter	1.9	3.5[a]
+ 5%	Flooded carbon α decay parameter	−0.4	−1.8[a]
+ 5%	Autochthonous v decay parameter	0.46	0.4[a]
+ 5%	Autochthonous α parameter	−0.2	−0.4[a]
+ 5%	Allochthonous v decay parameter	1.8	0.9[a]
+ 5%	Allochthonous α decay parameter	−0.5	−0.6[a]
+ 5%	Ratio of CH_4 to CO_2 production		5.0
Factors affecting internal fate/transport			
+ 5%	Baseline fraction of CH_4 production that gets internally oxidized or emitted via turbines (0.8 in Equation 6)		−27
+ 5%	Bubble dissolution rate		−1.8
+ 5%	Plant emissions (as % of eb + diff)		−0.7

Note. Results of the sensitivity analysis where individual parameters or inputs were increased by 5%. Results show the mean change in predicted CH_4 ebullition and diffusion. Reservoir age fixed at 50 years, unless otherwise noted.
[a]Reservoir age fixed at 1 year to analyze effect on young reservoirs.

0.4% and 1.9% increase in estimated ebullition plus diffusion (respectively). ResME is less sensitive to changing the α decay parameter, where a 5% increase in the α decay parameter for autochthonous and allochthonous carbon results in a −0.2%, and −0.5% change in emissions for each carbon source, respectively.

The effect of changing v and α for flooded carbon depends on the reservoir age, and the effect is larger when the reservoir is younger. Right after reservoir creation, increasing α (a proxy for average carbon lifetime) decreases CH_4 emissions in the short term, as flooded biomass carbon takes longer to break down. Conversely, raising v makes carbon less recalcitrant, which will increase CH_4 emissions. However, the effect changes when the reservoir is 50 years old. At 50 years, a higher α means there is more carbon left to decompose, so raising α raises average CH_4 emissions slightly. Raising v to make carbon less recalcitrant means more of the carbon will have decomposed at 50 years, thus lowering average CH_4 emissions.

Overall, ResME is most sensitive to changing the parameters governing CH_4 fate and transport within the reservoir, since these mechanisms act on CH_4 produced from all carbon types. In particular, ResME is very sensitive to a change in the baseline fraction (0.8, Equation 6) of produced CH_4 that gets internally oxidized or emitted via turbines (or immediately downstream of turbines). Increasing bubble dissolution also decreases ebullition plus diffusion, but at a much lower rate than changing the baseline oxidation level. The model's sensitivity to internal oxidation rates demonstrates that future work should focus on whole-reservoir methane budgets to reduce the uncertainty in this value.

Overall, the sensitivity test shows that ResME is reasonably robust against small changes in parameter input values aside from the fraction of methane oxidized or released through turbines. A 5% increase in parameter input value produces a 5% or smaller increase in surface CH_4 emissions estimates, for all input parameters except the baseline fraction of CH_4 production that gets internally oxidized. However, we do note that in some cases expected uncertainty in parameter input values may be much larger than 5%.

4.2. Uncertainty

Methane production and the dynamics of aquatic ecosystems are inherently complex, and ResME model results, as well as the field observations used for comparison, contain significant uncertainty. Of all the parameters and estimations that go into ResME, carbon input estimates are some of the most significant and uncertain. In particular, allochthonous POC and DOC estimates have high uncertainty: the prediction interval for POC as % of sediment matter (alpha = 0.05) is roughly order-of-magnitude, and the prediction interval for DOC as fraction of TOC is, on average, ±50% of the predicted fraction. Furthermore, the estimate of sediment concentration in riverine flow from WBM_sed contains high uncertainty, and WBM_Sed results compared with field measurements had an $r^2 = 0.66$ on a log-log scale (Cohen et al., 2013). The mean autochthonous primary production value per reservoir trophic status is estimated based on data from multiple reservoirs (Kimmel et al., 1990), where the standard deviation for each trophic status estimate is roughly ±35%. The relatively large uncertainty in autochthonous and allochthonous carbon inputs highlights the need for more robust methods of predicting these parameters.

ResME output was highly sensitive to several other parameters that are based on limited field-based estimations and thus uncertain. These include the ratio of CH_4 to CO_2 production from organic matter decay, the baseline fraction of CH_4 that gets internally oxidized, the fraction of autochthonous carbon that settles to the sediment, and autochthonous carbon decay. ResME uses the same parameters for each of these across all reservoirs, but there is likely substantial variation. Furthermore, since there are limited studies on carbon decay for multiple carbon types in anoxic environments, the ResME parameters are based on one study (Grasset et al., 2018) and this study yields a faster initial decay for allochthonous carbon compared with autochthonous carbon (though higher long-term recalcitrance). Future work should focus on more detailed estimates of autochthonous and allochthonous carbon decay in anoxic environments. Future model enhancements could allow for reservoir-specific parameters, though such specificity would need to be simple enough to apply on a global scale.In addition to the model uncertainty, the field estimates of methane ebullition and diffusion to which we compare the model also have substantial uncertainty (see discussion in Section 6.0 below).

The magnitude of methane released immediately following reservoir creation can be quite high compared with baseline emissions (Abril et al., 2005; Barros et al., 2011; Tremblay et al., 2005; Venkiteswaran et al., 2013) and is an additional source of uncertainty in global releases. The potential importance of this post-construction pulse of CH_4 has not yet been quantified because previous efforts to estimate CH_4 emissions from reservoirs have not modeled emissions changes over time. While ResME can model emissions over time, lack of field measurements for young reservoirs makes it difficult to determine how well ResME reproduces CH_4 emissions after reservoir construction. We found only eight studies (from reservoirs in South America, Canada, Eastern Europe, and Southeast Asia) with CH_4 emissions measurements within the first 10 years after reservoir creation and compared them to ResME model predictions (Figure S7 in Supporting Information S1). ResME is able to reasonably predict change in CH_4 emissions over time for several of the reservoirs, but it greatly underestimates emissions compared to measurements for other reservoirs. More measurements are needed to characterize how well ResME performs for young reservoirs, and to quantify the full atmospheric methane burden from newly flooded biomass.

5. Global CH_4 Emissions From Hydroelectric Reservoirs

There are 2,462 hydropower reservoirs in the GRanD global database (Figure 4), and collectively these reservoirs represent approximately 287,000 km^2 of surface area. To apply ResME on the global scale, we made simplifying assumptions about sediment temperature and reservoir trophic status. To calculate sediment temperature without bathymetric information, we assumed reservoir sediments were equally split between hypolimnetic and epilimnetic temperatures. This assumption should introduce limited error since our sensitivity analysis showed that ResME was relatively insensitive to changing the ratio of epilimnetic to hypolimnetic sediments. Estimating trophic status on a global scale is still difficult to achieve, though some progress is being made. Recent work

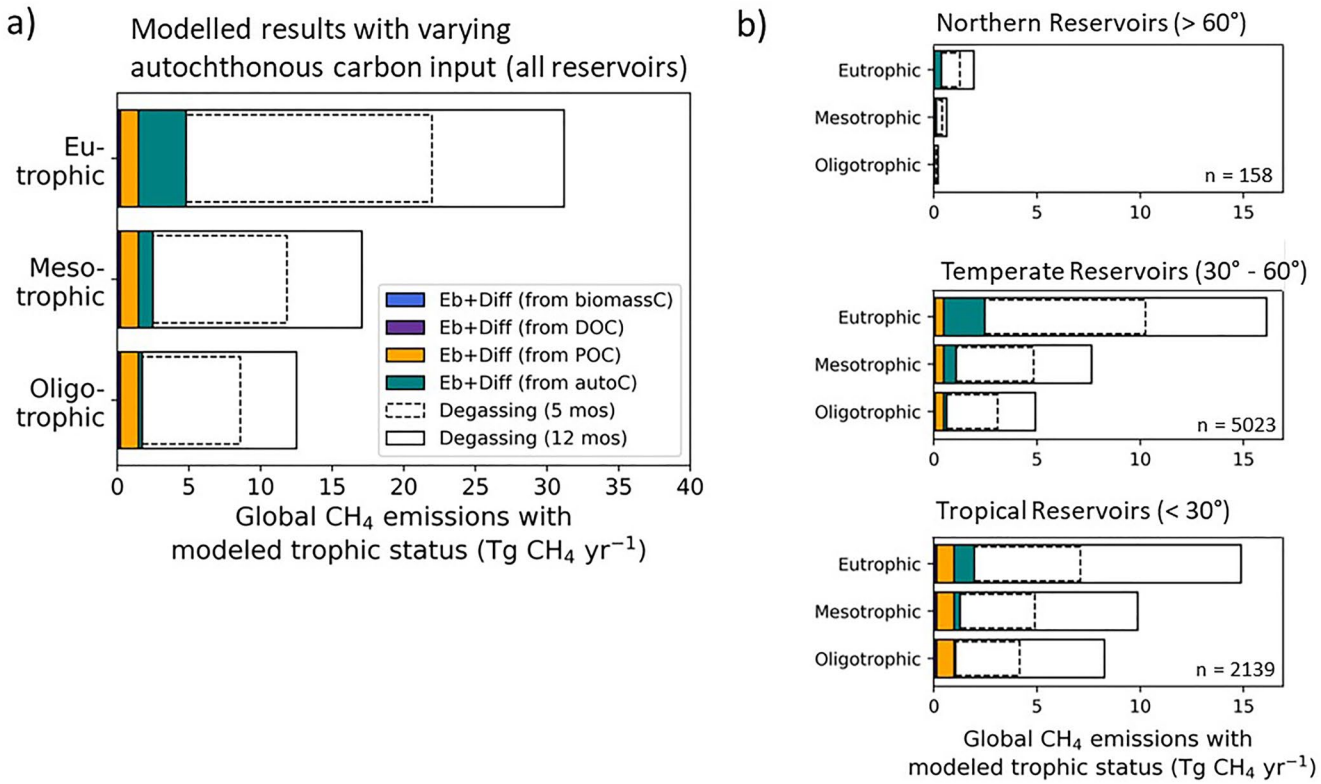

Figure 8. (a) Modeled global reservoir CH_4 emissions assuming all reservoirs are eutrophic (top bar), mesotrophic (middle bar), or oligotrophic (bottom bar). Contributions to methane emissions come from ebullition and diffusion fueled by five carbon sources: flooded biomass, allochthonous dissolved organic carbon (DOC), allochthonous particulate organic carbon, and autochthonous carbon (where flooded biomass and allochthonous DOC contributions are minimal). Maximum possible degassing emissions are equal to white bar outlined in solid black line; degassing emissions limited to 5 months shown in white bar outlined by dashed black line. (b) Modeled global reservoir CH_4 emissions based on latitudinal band, with same trophic status assumptions and legend as Figure 8a.

using MERIS full-resolution full-swath global data to estimate chlorophyll *a* concentrations (Sayers et al., 2021) found that observed water bodies were roughly equally split between typical chlorophyll *a* values for oligotrophic, mesotrophic, and eutrophic systems (based on trophic categories in Likens, 1975). We therefore assume annual emissions are the average emissions between oligotrophic, mesotrophic, and eutrophic systems. We also calculate lower and upper bounds for CH_4 emissions assuming all reservoirs are either oligotrophic or eutrophic, respectively. Since 10 of the reservoirs account for 26% of the total surface area, we used literature estimates of reservoir trophic status to assign fixed values of primary production to these largest systems (Table S4 in Supporting Information S1). Following Deemer et al., 2016, we excluded Lakes Victoria, Baikal, and Ontario as these large systems are natural lakes modified with hydropower facilities.

Our model results indicate that existing hydropower facilities emit 2.8 ± 0.2 Tg CH_4-C yr^{-1} via ebullition, diffusion, and plants. We estimate the mean and standard deviation using residual bootstrapping with 1,000 iterations (Efron & Tibshirani, 1993). Estimated uncertainty is much larger, see Section 4.2 above. Maximum potential emissions from turbine degassing are estimated as an additional 11 ± 4 Tg CH_4-C yr^{-1} assuming all reservoirs stratify for the five warmest months and 20% of released methane is oxidized prior to entering the atmosphere (where standard deviation comes from averaging output from the three trophic statuses). Potential turbine degassing jumps to 17 ± 7 Tg CH_4-C yr^{-1} if we assume all reservoirs are stratified year-round, which is a conservative upper-limit since many reservoirs experience periodic mixing. Since not all reservoirs in GRanD have turbine intakes within the hypolimnion, the true global emissions from turbine outlets are likely lower. We can estimate a lower bound on potential CH_4 emissions by assuming all reservoirs are oligotrophic, which yields 2 Tg CH_4-C yr^{-1} from surface emissions and 6 Tg CH_4-C yr^{-1} potential emissions from turbines (assuming emissions occur over a 5 month period and all dams draw water from the hypolimnion) (Figure 8a). The upper bound (assuming all reservoirs are eutrophic) is 5 Tg CH_4-C yr^{-1} and 17 Tg CH_4-C yr^{-1} from turbines. We also note that

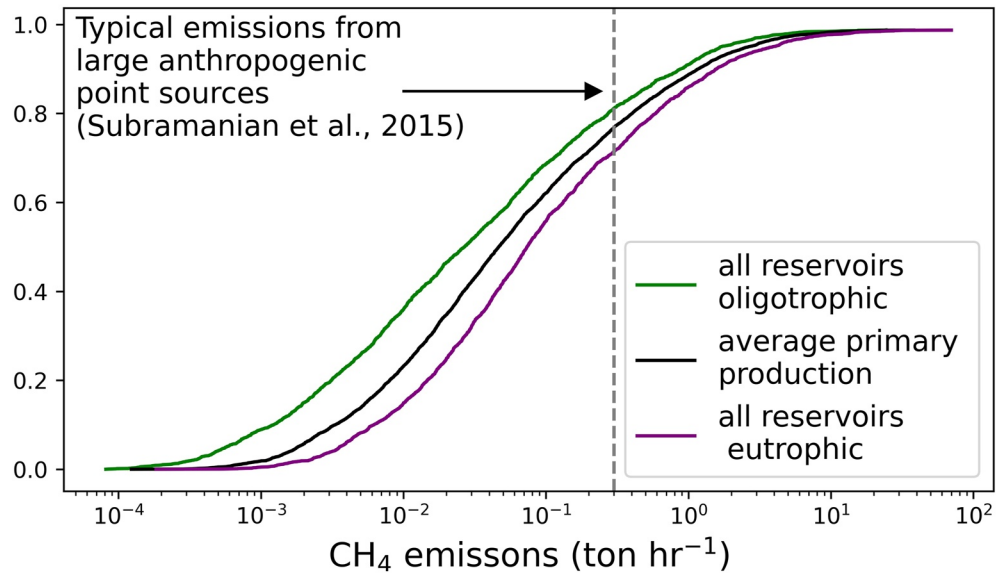

Figure 9. Cumulative frequency distributions for modeled maximum potential turbine CH_4 emissions assuming mean trophic status and 5-month stratification (black line), assuming all reservoirs are oligotrophic (green line), or assuming all reservoirs are eutrophic (purple line). For comparison, the gray dashed line shows methane (CH_4) emissions from a large anthropogenic point source, defined as 0.3 t CH_4/hr (Subramanian et al., 2015).

hydropower reservoirs (excluding Lakes Victoria, Baikal, and Ontario) make up 82% of total reservoir surface area in GRanD, and GRanD is not exhaustive, so global surface emissions from all reservoirs are potentially higher than ResME estimates.

ResME results also allow us to look at the methane contributions from reservoirs in different latitudinal bands (Figure 8b). Allochthonous carbon inputs contribute much more to total ebullition and diffusion emissions than autochthonous carbon inputs in tropical systems compared with temperate and northern systems (ratio of allochthonous to autochthonous-fueled methane emissions are 0.43, 0.17, and 0.02 for tropical, temperate, and northern latitudes, respectively), reflecting higher riverine carbon transport in tropical systems (as modeled by WBMSed). The different latitudinal bands also demonstrate that potential turbine emissions are more uniform year-round in tropical systems than temperate systems. In temperate systems 5 months of emissions during the warm season contributes a higher fraction of potential annual emissions than in tropical systems. This is to be expected given the more uniform year-round temperatures in tropical systems.

Turbines are potentially large point sources. For example, 24% of reservoirs have maximum potential downstream emissions higher than anthropogenic super-emitters, defined as sources exceeding 0.3 t CH_4/hr by Subramanian et al., 2015 (estimated by averaging output from oligotrophic, mesotrophic, and eutrophic scenarios and assuming reservoirs stratify for a 5-month period) (Figure 9). If all GRanD reservoirs were either oligotrophic or eutrophic, 18% or 29% would exceed 0.3 t/hr. Note that these figures represent average turbine methane emission rates over a 5-month period, and peak emissions could be higher depending on temporal dynamics. Table S5 in Supporting Information S1 contains a list of the top 20 CH_4 emitting reservoirs (based on downstream emissions), with estimations for maximum potential downstream emissions assuming year-round stratification and downstream emissions assuming a 5-month stratification period during warmest months and ebullitive + diffusive surface emissions.

6. Future Research Needs to Reduce Uncertainty in Emissions Estimates

ResME represents an important step forward in reservoir emissions modeling because the biogeochemical framework allows for a more detailed understanding of emissions drivers. However, ResME (as well as other empirical models of CH_4 emissions) have large uncertainties. While these uncertainties are to be expected in complex, dynamic ecosystems such as reservoirs, significant reductions in uncertainty would help better constrain the potential carbon benefits from hydroelectric power as well as CH_4 source-attribution in the global CH_4 budgets.

Some keys to reducing ResME uncertainty are to improve allochthonous POC loading estimates, add turbine intake depth information, increase sampling frequency and spatial coverage in field campaigns, increase studies of newly flooded reservoirs, and potentially use satellite CH_4 measurements to constrain downstream emissions.

Dam design (e.g., turbine intake depth) greatly influences potential downstream emissions, yet the GRanD database lacks information on the relative water intake height for each dam. Updating GRanD to contain this information would allow us to narrow the range of estimated CH_4 degassing at turbines. Additional studies to measure turbine degassing from deep-intake turbines would also help reduce the uncertainty around ResME estimates for turbine degassing, since we currently only have four studies measuring emissions from deep-intake turbines.

Uncertainty in the estimates of CH_4 emissions from hydropower reservoirs, particularly recently-flooded reservoirs, could be reduced through more robust field campaigns to accurately estimate surface emissions. Recent work shows that accurately capturing the temporal and spatial heterogeneity in diffusive and ebullitive methane fluxes across seasons requires a significant investment of time and resources (Linkhorst et al., 2020; Paranaiba et al., 2021; Wik et al., 2016). Given the practical constraints on such extensive sampling, the large majority of studies do not attain this rigorous requirement. More extensive field campaigns could provide more accurate results, though such campaigns can be prohibitively time intensive. More CH_4 emissions estimates from newly flooded reservoirs are especially important given the potential for very large emissions from these systems, and the current lack of data from systems less than 10 years old. More field campaigns in river deltas, where allochthonous POC is likely to settle and where previous measurements have found significantly higher CH_4 emissions, would also improve overall estimates of reservoir CH_4 emissions.

Measured estimates of reservoir CH_4 emissions could also be improved through remote sensing data from satellites. The TROPOMI instrument launched in October 2017 provides global daily mapping of atmospheric CH_4 columns at 5.5 × 7 km pixel resolution but observation over water bodies is limited to the sunglint mode (Hasekamp et al., 2019; Lorente et al., 2021; Veefkind et al., 2012). One could still detect CH_4 emissions from reservoirs by observing the enhancements transported over land, and quantify the source using inverse methods (Jacob et al., 2016; Maasakkers et al., 2019). The point source emissions from turbines could be detected and quantified by a new class of satellite instruments including GHGSat and PRISMA that observe atmospheric CH_4 plumes with ∼30 m pixel resolution and detection thresholds in the range 0.1–0.5 t hr^{-1} for ideal circumstances (Guanter et al., 2021; Jervis et al., 2021; Varon et al., 2019). Initial attempts to find turbine-related CH_4 plumes in TROPOMI yielded promising results near the Lom Pangar dam in Cameroon. Figure 10 shows 2 days in December with a clear CH_4 enhancement over the dam. Sentinel-2 visual imagery from December 25 shows that water is flowing through the dam during that time period (Gascon et al., 2017). The GHGSat satellite instrument targeted at point source observations was also able to detect a CH_4 plume from turbine outgassing over the Lom Pangar dam (Jervis et al., 2021). Assuming a source rate detection threshold of 0.25 t hr^{-1} from satellite instruments, 25% of the GRanD reservoirs could have detectable turbine fluxes (if turbines pull from a CH_4-rich hypolimnion).

7. Conclusions

ResME's estimate of 2.8 Tg CH4-C yr^{-1} emitted from hydropower facilities via ebullition and diffusion falls within the range of previously estimated emissions from hydropower reservoir surfaces, which estimated emissions around 3–4.4 Tg CH_4 yr^{-1} (Barros et al., 2011; Deemer et al., 2016; Li & Zhang, 2014). ResME estimates of maximum possible turbine degassing at 11 Tg CH_4-C yr^{-1} is also comparable to a previous estimate of 7.4 Tg CH_4 yr^{-1} (Li & Zhang, 2014). However, large uncertainties remain, and substantial work will be needed to reduce this uncertainty. The process focus of ResME allows for a deeper understanding of the factors affecting CH_4 emissions from hydropower. The relative importance of different carbon inputs to methane emissions also vary across the globe, with tropical latitude reservoirs typically having a higher relative fraction of methane produced from allochthonous carbon inflows. As our results have shown, data on turbine intake depth is the most important factor for predicting hydropower methane emissions, pointing to the need for global records on hydropower reservoir turbine depths.

Contributions from newly flooded carbon can substantially increase CH_4 emissions in the few years after reservoir creation, though more field measurements are needed to reduce uncertainty. Improving estimates for newly flooded reservoirs will be particularly important in the future, since there were 3,700 new hydropower dams

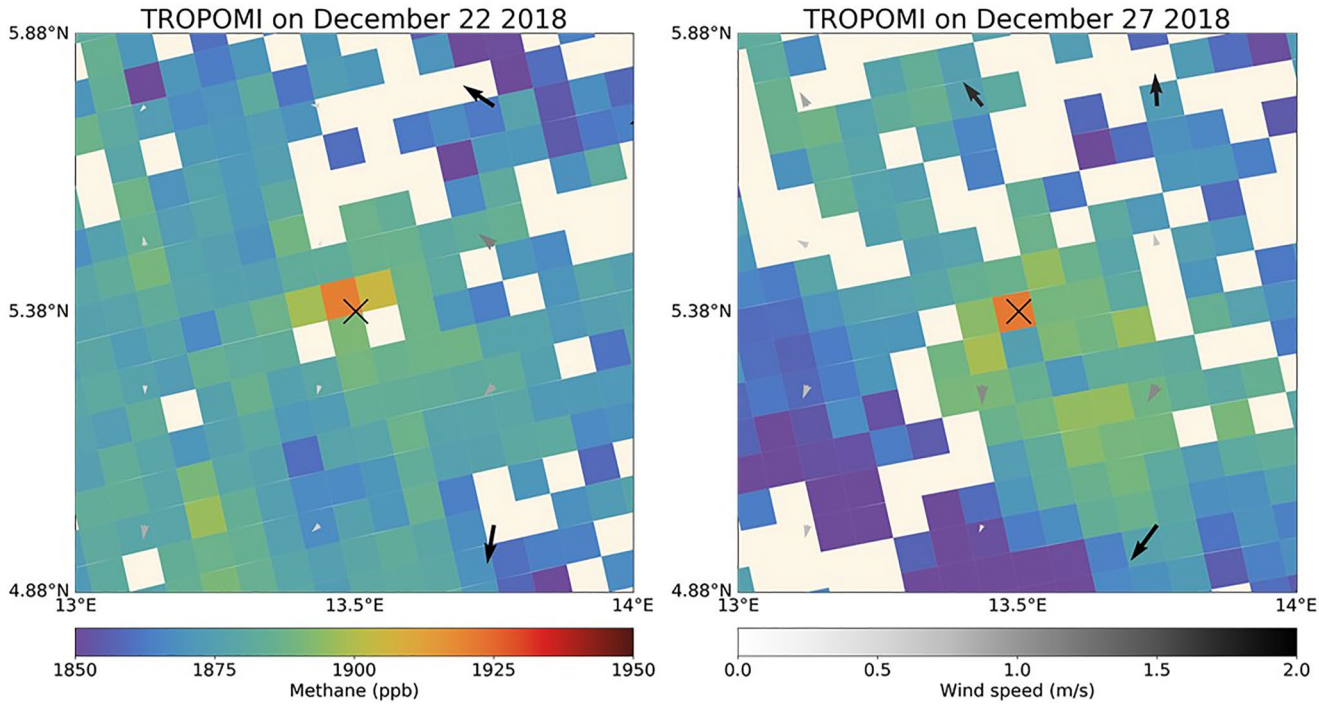

Figure 10. TROPOMI methane data show an enhancement over the Lom Pangar dam (indicated by the cross) in Cameroon in December 2018. Also shown are 10 m wind vectors from the GEOS-FP reanalysis product (Molod et al., 2012).

planned as of 2015 (Zarfl et al., 2015). Predicting, and potentially mitigating, the CH_4 emissions from these new systems will require more detailed data describing how CH_4 emissions evolve after reservoir creation.

Data Availability Statement

All model code and input data necessary to run ResME are available in a GitHub release (https://github.com/kyleb-delwiche/ResME) and on Zenodo (https://doi.org/10.5281/zenodo.6930246). Global CH_4 emissions estimates from hydropower are provided on Zenodo (https://doi.org/10.5281/zenodo.6360747). Emissions are divided into reservoir surface emissions (ebullition + diffusion) and potential dam emissions, and are provided for reservoirs in the GRanD database. Reservoir locations are reported as the reservoir latitude and longitude in the GRanD database (https://globaldamwatch.org/grand/). SibCASA carbon pool data are available at https://daac.ornl.gov/cgi-bin/dsviewer.pl?ds_id=1225. MERRA2 annual temperature data is available at https://disc.gsfc.nasa.gov/datasets?project=MERRA-2. TROPOMI data are available at https://ftp.sron.nl/open-access-data-2/TROPOMI/tropomi/ch4/14_14_Lorente_et_al_2020_AMTD/. Information for how to download WBMSed model results available at https://sdml.ua.edu/datasets-2/. GEOS-FP wind data are available at: gmao.gsfc.nasa.gov/GMAO_products. Sentinel- 2 data are available from the Copernicus Open Access Hub (https://scihub.copernicus.eu), and data used here was obtained from the Sentinel Hub EO Browser (https://apps.sentinel-hub.com/eo-browser/).

Acknowledgments
This work was supported by the Harvard Climate Change Solutions fund and the NASA Carbon Monitoring System. We acknowledge support from the Gordon and Betty Moore Foundation (Grant GBMF5439, "Advancing Understanding of the Global Methane Cycle"; Stanford University). Part of this research was carried out at the Jet Propulsion Laboratory, California Institute of

References

Abril, G., Guérin, F., Richard, S., Delmas, R., Galy-Lacaux, C., Gosse, P., et al. (2005). Carbon dioxide and methane emissions and the carbon budget of a 10-year old tropical reservoir (Petit Saut, French Guiana). *Global Biogeochemical Cycles*, *19*(4), B2457. https://doi.org/10.1029/2005GB002457

Baines, S. B., & Pace, M. L. (1994). Relationships between suspended particulate matter and sinking flux along a trophic gradient and implications for the fate of planktonic primary production. Canadian Journal of Fisheries and Aquatic Sciences. *Journal Canadien Des Sciences Halieutiques et Aquatiques*, *51*(1), 25–36. https://doi.org/10.1139/f94-005

Barros, N., Cole, J. J., Tranvik, L. J., Prairie, Y. T., Bastviken, D., Huszar, V. L. M., et al. (2011). Carbon emission from hydroelectric reservoirs linked to reservoir age and latitude. *Nature Geoscience*, *4*(9), 593–596. https://doi.org/10.1038/ngeo1211

Bastviken, D., Cole, J. J., Pace, M. L., & Van de Bogert, M. C. (2008). Fates of methane from different lake habitats: Connecting whole-lake budgets and CH_4 emissions. *Journal of Geophysical Research*, *113*(G2). https://doi.org/10.1029/2007JG000608

Technology, under a contract with the National Aeronautics and Space Administration. The authors thank the team that realized the TROPOMI instrument and its data products, consisting of the partnership between Airbus Defence and Space Netherlands, KNMI, SRON, and TNO, commissioned by NSO and ESA. Sentinel-5 Precursor is part of the EU Copernicus program, Copernicus Sentinel-5P data (2018) have been used. Funding support to Harrison for this work included a Stanford University Cox visiting professorship and NSF DISES #2109259. We thank Sagy Cohen for providing WBMSed simulation results (https://sdml.ua.edu/datasets-2/). Authors thank the anonymous reviewers for their valuable comments.

Bastviken, D., Tranvik, L. J., Downing, J. A., Crill, P. M., & Enrich-Prast, A. (2011). Freshwater methane emissions offset the continental carbon sink. *Science*, *331*(6013), 50. https://doi.org/10.1126/science.1196808

Berman, T., Yacobi, Y. Z., Parparov, A., & Gal, G. (2010). Estimation of long-term bacterial respiration and growth efficiency in Lake Kinneret. *FEMS Microbiology Ecology*, *71*(3), 351–363. https://doi.org/10.1111/j.1574-6941.2009.00822.x

Bižić, M., Klintzsch, T., Ionescu, D., Hindiyeh, M. Y., Günthel, M., Muro-Pastor, A. M., et al. (2020). Aquatic and terrestrial cyanobacteria produce methane. *Science Advances*, *6*(3), eaax5343. https://doi.org/10.1126/sciadv.aax5343

Bogard, M. J., del Giorgio, P. A., Boutet, L., Chaves, M. C. G., Prairie, Y. T., Merante, A., & Derry, A. M. (2014). Oxic water column methanogenesis as a major component of aquatic CH_4 fluxes. *Nature Communications*, *5*(1), 5350. https://doi.org/10.1038/ncomms6350

Borrel, G., Jézéquel, D., Biderre-Petit, C., Morel-Desrosiers, N., Morel, J.-P., Peyret, P., et al. (2011). Production and consumption of methane in freshwater lake ecosystems. *Research in Microbiology*, *162*(9), 832. https://doi.org/10.1016/j.resmic.2011.06.004

Boudreau, B. P., Arnosti, C., Jørgensen, B. B., & Canfield, D. E. (2008). Comment on "Physical model for the decay and preservation of marine organic carbon". *Science*, *319*(5870), 1616. https://doi.org/10.1126/science.1148589

Boudreau, B. P., & Ruddick, B. R. (1991). On a reactive continuum representation of organic matter diagenesis. *American Journal of Science*, *291*(5), 507–538. https://doi.org/10.2475/ajs.291.5.507

Boylan, J. W., & Russell, A. G. (2006). PM and light extinction model performance metrics, goals, and criteria for three-dimensional air quality models. *Atmospheric Environment*, *40*(26), 4946–4959. https://doi.org/10.1016/j.atmosenv.2005.09.087

C3S: Copernicus Climate Change Service. (2017). Search ERA5: Fifth generation of ECMWF atmospheric reanalyses of the global climate. Copernicus climate change Service climate data Store (CDS). Retrieved from https://cds.climate.copernicus.eu/cdsapp%23%21/home. (accessed through Google Earth Engine, December 2021).

Casper, P., Maberly, S. C., Hall, G. H., & Finlay, B. J. (2000). Fluxes of methane and carbon dioxide from a small productive lake to the atmosphere. *Biogeochemistry*, *49*(1), 1–19. https://doi.org/10.1023/A:1006269900174

Catalan, N., Casas-Ruiz, J. P., von Schiller, D., Proia, L., Obrador, B., Zwirnmann, E., & Marce, R. (2017). Biodegradation kinetics of dissolved organic matter chromatographic fractions in an intermittent river. *Journal of Geophysical Research: Biogeosciences*, *122*(1), 131–144. https://doi.org/10.1002/2016JG003512

Chanudet, V., Descloux, S., Harby, A., Sundt, H., Hansen, B. H., Brakstad, O., et al. (2011). Gross CO_2 and CH_4 emissions from the Nam Ngum and Nam Leuk sub-tropical reservoirs in Lao PDR. *Science of the Total Environment*, *409*(24), 5382–5391. https://doi.org/10.1016/j.scitotenv.2011.09.018

Cohen, S., Kettner, A. J., Syvitski, J. P. M., & Fekete, B. M. (2013). WBMsed, a distributed global-scale riverine sediment flux model: Model description and validation. *Computers & Geosciences*, *53*, 80–93. https://doi.org/10.1016/j.cageo.2011.08.011

Conrad, R. (2005). Quantification of methanogenic pathways using stable carbon isotopic signatures: A review and a proposal. *Organic Geochemistry*, *36*(5), 739–752. https://doi.org/10.1016/j.orggeochem.2004.09.006

Darchambeau, F., Thys, I., Leporcq, B., Hoffmann, L., & Descy, J.-P. (2005). Influence of zooplankton stoichiometry on nutrient sedimentation in a lake system. *Limnology and Oceanography*, *50*(3), 905–913. https://doi.org/10.4319/lo.2005.50.3.0905

Deemer, B. R., Harrison, J. A., Li, S., Beaulieu, J. J., DelSontro, T., Barros, N., et al. (2016). Greenhouse gas emissions from reservoir water surfaces: A new global synthesis. *BioScience*, *66*(11), 949–964. https://doi.org/10.1093/biosci/biw117

Deemer, B. R., & Holgerson, M. A. (2021). Drivers of methane flux differ between lakes and reservoirs, complicating global upscaling efforts. *Journal of Geophysical Research: Biogeosciences*, *126*(4), e2019JG005600. https://doi.org/10.1029/2019JG005600

DelSontro, T., Beaulieu, J. J., & Downing, J. A. (2019). Greenhouse gas emissions from lakes and impoundments: Upscaling in the face of global change. *Limnology and Oceanography Letters*, *3*(3), 64–75. https://doi.org/10.1002/lol2.10073

DelSontro, T., McGinnis, D. F., Wehrli, B., & Ostrovsky, I. (2015). Size does matter: Importance of large bubbles and small-scale hot spots for methane transport. *Environmental Science & Technology*, *49*(3), 1268–1276. https://doi.org/10.1021/es5054286

Delwiche, K. B., & Hemond, H. F. (2017). Methane bubble size distributions, flux, and dissolution in a freshwater lake. *Environmental Science & Technology*, *51*(23), 13733–13739. https://doi.org/10.1021/acs.est.7b04243

De Vicente, I., Rueda, F., Cruz-Pizarro, L., & Morales-Baquero, R. (2008). Implications of seston settling on phosphorus dynamics in three reservoirs of contrasting trophic state. *Fundamental and Applied Limnology/Archiv Für Hydrobiologie*, *170*(4), 263–272. https://doi.org/10.1127/1863-9135/2008/0170-0263

Efron, B., & Tibshirani, R. (1993). *An introduction to the bootstrap*. Chapman & Hall/CRC. ISBN 0-412-04231-2.

Etminan, M., Myhre, G., Highwood, E. J., & Shine, K. P. (2016). Radiative forcing of carbon dioxide, methane, and nitrous oxide: A significant revision of the methane radiative forcing. *Geophysical Research Letters*, *43*(24), 12614–12623. https://doi.org/10.1002/2016gl071930

Fearnside, P. M. (2002). Greenhouse gas emissions from a hydroelectric reservoir (Brazil's Tucurui dam) and the energy policy implications. *Water, Air, and Soil Pollution*, *133*, 69–96. https://doi.org/10.1023/A:1012971715668

Fernández, E. J., Peeters, F., & Hofmann, H. (2014). Importance of the autumn overturn and anoxic conditions in the hypolimnion for the annual methane emissions from a temperate lake. *Environmental Science & Technology*, *48*(13), 7297–7304. https://doi.org/10.1021/es4056164

Gascon, F., Bouzinac, C., Thépaut, O., Jung, M., Francesconi, B., Louis, J., et al. (2017). Copernicus sentinel-2A calibration and products validation status. *Remote Sensing*, *9*(6), 584. https://doi.org/10.3390/rs9060584

Golub, M., Thiery, W., Marcé, R., Pierson, D., Vanderkelen, I., Mercado, D., et al. (2022). A framework for ensemble modelling of climate change impacts on lakes worldwide: The ISIMIP lake sector, Geosci [preprint]. Model Development Discussion. https://doi.org/10.5194/gmd-2021-433 .

Gorelick, N., Hancher, M., Dixon, M., Ilyushchenko, S., Thau, D., & Moore, R. (2017). Google Earth Engine: Planetary-scale geospatial analysis for everyone. *Remote Sensing of Environment*, *202*, 18–27. https://doi.org/10.1016/j.rse.2017.06.031

Grasset, C., Mendonça, R., Villamor Saucedo, G., Bastviken, D., Roland, F., & Sobek, S. (2018). Large but variable methane production in anoxic freshwater sediment upon addition of allochthonous and autochthonous organic matter. *Limnology and Oceanography*, *63*(4), 1488–1501. https://doi.org/10.1002/lno.10786

Grossart, H.-P., Frindte, K., Dziallas, C., Eckert, W., & Tang, K. W. (2011). Microbial methane production in oxygenated water column of an oligotrophic lake. *Proceedings of the National Academy of Sciences of the United States of America*, *108*(49), 19657–19661. https://doi.org/10.1073/pnas.1110716108

Guanter, L., Irakulis-Loitxate, I., Gorroño, J., Sánchez-García, E., Cusworth, D. H., Varon, D. J., et al. (2021). Mapping methane point emissions with the PRISMA spaceborne imaging spectrometer. *Remote Sensing of Environment*, *265*, 112671. https://doi.org/10.1016/j.rse.2021.112671

Gudasz, C., Bastviken, D., Premke, K., Steger, K., & Tranvik, L. J. (2012). Constrained microbial processing of allochthonous organic carbon in boreal lake sediments. *Limnology and Oceanography*, *57*(1), 163–175. https://doi.org/10.4319/lo.2012.57.1.0163

Günthel, M., Donis, D., Kirillin, G., Ionescu, D., Bizic, M., McGinnis, D. F., et al. (2019). Contribution of oxic methane production to surface methane emission in lakes and its global importance. *Nature Communications*, *10*(1), 5497. https://doi.org/10.1038/s41467-019-13320-0

Hall, B. D., & St. Louis, V. L. (2004). Methylmercury and total mercury in plant litter decomposing in upland forests and flooded landscapes. *Environmental Science & Technology*, *38*(19), 5010–5021. https://doi.org/10.1021/es049800q

Hanson, P. C., Pace, M. L., Carpenter, S. R., Cole, J. J., & Stanley, E. H. (2015). Integrating landscape carbon cycling: Research needs for resolving organic carbon budgets of lakes. *Ecosystems*, *18*(3), 363–375. https://doi.org/10.1007/s10021-014-9826-9

Harrison, J., Prairie, Y. T., Mercier-Blais, S., & Soued, C. (2021). Year-2020 global distribution and pathways of reservoir methane and carbon dioxide emissions according to the greenhouse gas from reservoirs (G-res) model. *Global Biogeochemical Cycles*, *35*(6), e2020GB006888. https://doi.org/10.1029/2020GB006888

Hasekamp, O., Lorente, A., Hu, H., Butz, A., Aan de Brugh, J., & Landgraf, J. (2019). Algorithm Theoretical Baseline Document for Sentinel-5 Precursor Methane Retrieval (SRON-S5P- LEV2-RP-001, 2019). Retrieved from https://sentinel.esa.int/documents/247904/2476257/Sentinel-5P-TROPOMI-ATBD-Methane-retrieval

Huntzinger, D. N., Schwalm, C. R., Wei, Y., Cook, R. B., Michalak, A. M., Schaefer, K., et al. (2018). *NACP MsTMIP: Global 0.5-degree Model Outputs in Standard Format* (Version 1.0) [Dataset]. ORNL DAAC. https://doi.org/10.3334/ORNLDAAC/1225

Jacob, D. J., Turner, A. J., Maasakkers, J. D., Sheng, J., Sun, K., Liu, X., et al. (2016). Satellite observations of atmospheric methane and their value for quantifying methane emissions. *Atmospheric Chemistry and Physics*, *16*(22), 14371–14396. https://doi.org/10.5194/acp-16-14371-2016

Jansson, M., Persson, L., De Roos, A. M., Jones, R. I., & Tranvik, L. J. (2007). Terrestrial carbon and intraspecific size-variation shape lake ecosystems. *Trends in Ecology & Evolution*, *22*(6), 316–322. https://doi.org/10.1016/j.tree.2007.02.015

Jervis, D., McKeever, J., Durak, B. O. A., Sloan, J. J., Gains, D., Varon, D. J., et al. (2021). The GHGSat-D imaging spectrometer. *Atmospheric Measurement Techniques*, *14*(3), 2127–2140. https://doi.org/10.5194/amt-14-2127-2021

Jones, R. I. (1992). The influence of humic substances on lacustrine planktonic food chains. *Hydrobiologia*, *229*(1), 73–91. https://doi.org/10.1007/BF00006992

Kankaala, P., Huotari, J., Peltomaa, E., Saloranta, T., & Ojala, A. (2006). Methanotrophic activity in relation to methane efflux and total heterotrophic bacterial production in a stratified, humic, boreal lake. *Limnology and Oceanography*, *51*(2), 1195–1204. https://doi.org/10.4319/lo.2006.51.2.1195

Kankaala, P., Taipale, S., Nykänen, H., & Jones, R. I. (2007). Oxidation, efflux, and isotopic fractionation of methane during autumnal turnover in a polyhumic, boreal lake. *Journal of Geophysical Research*, *112*(G2), G02033. https://doi.org/10.1029/2006jg000336

Kemenes, A., Forsberg, B. R., & Melack, J. M. (2007). Methane release below a tropical hydroelectric dam. *Geophysical Research Letters*, *34*(12), GB4007. https://doi.org/10.1029/2007GL029479

Kimmel, B. L., Lind, O. T., & Paulson, L. J. (1990). Reservoir primary production. In K. W. Thornton, B. K. Kimmel, & F. E. Payne (Eds.), *Reservoir limnology: Ecological perspectives* (pp. 133–193). John Wiley & Sons.

Koehler, B., & Tranvik, L. J. (2015). Reactivity continuum modeling of leaf, root, and wood decomposition across biomes. *Journal of Geophysical Research: Biogeosciences*, *120*(7), 1196–1214. https://doi.org/10.1002/2015JG002908

Koehler, B., von Wachenfeldt, E., Kothawala, D., & Tranvik, L. J. (2012). Reactivity continuum of dissolved organic carbon decomposition in lake water. *Journal of Geophysical Research*, *117*(G1), 141. https://doi.org/10.1029/2011JG001793

Lee, H., Chung, S., Ryu, I., & Choi, J. (2013). Three-dimensional modeling of thermal stratification of a deep and dendritic reservoir using ELCOM model. *Journal of Hydro-Environment Research*, *7*(2), 124–133. https://doi.org/10.1016/j.jher.2012.10.002

Lehner, B., Liermann, C. R., Revenga, C., Vörösmarty, C., Fekete, B., Crouzet, P., et al. (2011). High-resolution mapping of the world's reservoirs and dams for sustainable river-flow management. *Frontiers in Ecology and the Environment*, *9*(9), 494–502. https://doi.org/10.1890/100125

Li, S., & Zhang, Q. (2014). Carbon emission from global hydroelectric reservoirs revisited. *Environmental Science and Pollution Research International*, *21*(23), 13636–13641. https://doi.org/10.1007/s11356-014-3165-4

Likens, G. E. (1975). Primary production of Inland aquatic ecosystems. In R. W. Helmut Lieth (Ed.), *Primary productivity of the biosphere* (pp. 186–202). Springer-Verlag.

Linkhorst, A., Hiller, C., DelSontro, T. M., Azevedo, G., Barros, N., Mendonça, R., & Sobek, S. (2020). Comparing methane ebullition variability across space and time in a Brazilian reservoir. *Limnology and Oceanography*, *65*(7), 1623–1634. https://doi.org/10.1002/lno.11410

Lorente, A., Borsdorff, T., Butz, A., Hasekamp, O., Schneider, A., Wu, L., et al. (2021). Methane retrieved from TROPOMI: Improvement of the data product and validation of the first 2 years of measurements. *Atmospheric Measurement Techniques*, *14*(1), 665–684. https://doi.org/10.5194/amt-14-665-2021

Maasakkers, J. D., Jacob, D. J., Sulprizio, M. P., Scarpelli, T., Nesser, H., Sheng, J.-X., et al. (2019). Global distribution of methane emissions, emission trends, and OH concentrations and trends inferred from an inversion of GOSAT satellite data for 2010–2015. *Atmospheric Chemistry and Physics*, *19*(11), 7859–7881. https://doi.org/10.5194/acp-19-7859-2019

Matthews, C. J. D., Joyce, E. M., Louis, V. L. S., Schiff, S. L., Venkiteswaran, J. J., Hall, B. D., et al. (2005). Carbon dioxide and methane production in small reservoirs flooding upland boreal forest. *Ecosystems*, *8*(3), 267–285. https://doi.org/10.1007/s10021-005-0005-x

Mayr, M. G., Zimmermann, M., Dey, J., Brand, A., Wehrli, B., & Bürgmann, H. (2020). Growth and rapid succession of methanotrophs effectively limit methane release during lake overturn. *Communications Biology*, *3*(108), 1–9. https://doi.org/10.1038/s42003-020-0838-z

McGinnis, D. F., Greinert, J., Artemov, Y., Beaubien, S. E., & Wüest, A. (2006). Fate of rising methane bubbles in stratified waters: How much methane reaches the atmosphere? *Journal of Geophysical Research*, *111*(C9), C09007. https://doi.org/10.1029/2005jc003183

Mendonça, R., Müller, R. A., Clow, D., Verpoorter, C., Raymond, P., Tranvik, L. J., & Sobek, S. (2017). Organic carbon burial in global lakes and reservoirs. *Nature Communications*, *8*(1), 1694. https://doi.org/10.1038/s41467-017-01789-6

Meybeck, M. (1982). Carbon, nitrogen, and phosphorus transport by world rivers. *American Journal of Science*, *282*(4), 401–450. https://doi.org/10.2475/ajs.282.4.401

Meybeck, M., & Ragu, A. (2012). *GEMS-GLORI world river discharge database*. Laboratoire de Géologie Appliquée, Université Pierre et Marie Curie, Paris, France, PANGAEA. https://doi.org/10.1594/PANGAEA.804574

Mironov, D., Heise, E., Kourzeneva, E., Ritter, B., Schneider, N., & Terzhevik, A. (2010). Implementation of the lake parameterisation scheme FLake into the numerical weather prediction model COSMO.

Molod, A., Takacs, L., Suarez, M., Bacmeister, J., In-Sun, S., & Eichmann, A. (2012). The GEOS-5 Atmospheric General Circulation Model: Mean Climate and Development from MERRA to Fortuna (Technical Report Series on Global Modeling and Data Assimilation, Volume 28, 2012).

Moran, M. A., Benner, R., & Hodson, R. E. (1989). Kinetics of microbial degradation of vascular plant material in two wetland ecosystems. *Oecologia*, *79*(2), 158–167. https://doi.org/10.1007/BF00388472

Mostovaya, A., Hawkes, J. A., Koehler, B., Dittmar, T., & Tranvik, L. J. (2017). Emergence of the reactivity continuum of organic matter from kinetics of a multitude of individual molecular constituents. *Environmental Science & Technology*, *51*(20), 11571–11579. https://doi.org/10.1021/acs.est.7b02876

Noori, R., Asadi, N., & Deng, Z. (2019). A simple model for simulation of reservoir stratification. *Journal of Hydraulic Research*, *57*(4), 561–572. https://doi.org/10.1080/00221686.2018.1499052

Ostrovsky, I., McGinnis, D. F., Lapidus, L., & Eckert, W. (2008). Quantifying gas ebullition with echosounder: The role of methane transport by bubbles in a medium-sized lake: Measuring methane transport with bubbles. *Limnology and Oceanography: Methods*, *6*(2), 105–118. https://doi.org/10.4319/lom.2008.6.105

Ostrovsky, I., & Yacobi, Y. Z. (2010). Sedimentation flux in a large subtropical lake: Spatiotemporal variations and relation to primary productivity. *Limnology and Oceanography*, *55*(5), 1918–1931. https://doi.org/10.4319/lo.2010.55.5.1918

Paranaíba, J. R., Barros, N., Almeida, R. M., Linkhorst, A., Mendonça, R., Vale, R., et al. (2021). Hotspots of diffusive CO_2 and CH_4 emission from tropical reservoirs shift through time. *Journal of Geophysical Research: Biogeosciences*, *126*(4), e2020JG006014. https://doi.org/10.1029/2020jg006014

Park, H.-K., Byeon, M.-S., Shin, Y.-N., & Jung, D.-I. (2009). Sources and spatial and temporal characteristics of organic carbon in two large reservoirs with contrasting hydrologic characteristics. *Water Resources Research*, *45*(11), W11418. https://doi.org/10.1029/2009wr008043

Peeters, F., Fernandez, J. E., & Hofmann, H. (2019). Sediment fluxes rather than oxic methanogenesis explain diffusive CH_4 emissions from lakes and reservoirs. *Scientific Reports*, *9*(1), 243. https://doi.org/10.1038/s41598-018-36530-w

Prairie, Y. T., Alm, J., Harby, A., Mercier-Blais, S., & Nahas, R. (2017). The GHG Reservoir Tool (Gres) Technical documentation, UNESCO/IHA Research Project on the GHG Status of Freshwater Reservoirs. Version 1.13. Joint Publication of the UNESCO Chair in Global Environmental Change and the International Hydropower Association, 1.13.

Prairie, Y. T., Mercier-Blais, S., Harrison, J. A., Soued, C., del Giorgio, P., Harby, A., et al. (2021). A new modelling framework to assess biogenic GHG emissions from reservoirs: The G-res tool. *Environmental Modelling & Software*, *143*, 105117. https://doi.org/10.1016/j.envsoft.2021.105117

Rudd, J. W. M., & Hamilton, R. D. (1978). Methane cycling in a eutrophic shield lake and its effects on whole lake metabolism 1. *Limnology and Oceanography*, *23*(2), 337–348. https://doi.org/10.4319/lo.1978.23.2.0337

Sayers, M. J., Fahnenstiel, G. L., Shuchman, R. A., & Bosse, K. R. (2021). A new method to estimate global freshwater phytoplankton carbon fixation using satellite remote sensing: Initial results. *International Journal of Remote Sensing*, *42*(10), 3708–3730. https://doi.org/10.1080/01431161.2021.1880661

Schaefer, K., James Collatz, G., Tans, P., Scott Denning, A., Baker, I., Berry, J., et al. (2008). Combined simple biosphere/Carnegie-Ames-Stanford approach terrestrial carbon cycle model. *Journal of Geophysical Research*, *113*(G3), G03034. https://doi.org/10.1029/2007jg000603

Schmid, M., Ostrovsky, I., & McGinnis, D. F. (2017). Role of gas ebullition in the methane budget of a deep subtropical lake: What can we learn from process-based modeling? *Limnology and Oceanography*, *62*(6), 2674–2698. https://doi.org/10.1002/lno.10598

Schubert, C. J., Diem, T., & Eugster, W. (2012). Methane emissions from a small wind shielded lake determined by eddy covariance, flux chambers, anchored funnels, and boundary model calculations: A comparison. *Environmental Science & Technology*, *46*(8), 4515–4522. https://doi.org/10.1021/es203465x

Soued, C., & Prairie, Y. T. (2020). The carbon footprint of a Malaysian tropical reservoir: Measured versus modelled estimates highlight the underestimated key role of downstream processes. *Biogeosciences*, *17*(2), 515–527. https://doi.org/10.5194/bg-17-515-2020

Steinsberger, T., Wüest, A., & Müller, B. (2021). Net ecosystem production of lakes estimated from hypolimnetic organic carbon sinks. *Water Resources Research*, *57*(5). https://doi.org/10.1029/2020wr029473

Stepanenko, V. M., Machul'skaya, E. E., Glagolev, M. V., & Lykossov, V. N. (2011). Numerical modeling of methane emissions from lakes in the permafrost zone. *Izvestiya, Atmospheric and Oceanic Physics/Izvestiya Rossiiskoi Akademii Nauk: Fizika Atmosfery I Okeana*, *47*(2), 252–264. https://doi.org/10.1134/s0001433811020113

Subramanian, R., Williams, L. L., Vaughn, T. L., Zimmerle, D., Roscioli, J. R., Herndon, S. C., et al. (2015). Methane emissions from natural gas compressor stations in the transmission and storage sector: Measurements and comparisons with the EPA greenhouse gas reporting program protocol. *Environmental Science & Technology*, *49*(5), 3252–3261. https://doi.org/10.1021/es5060258

Tan, Z., Zhuang, Q., & Walter Anthony, K. (2015). Modeling methane emissions from arctic lakes: Model development and site-level study. *Journal of Advances in Modeling Earth Systems*, *7*(2), 459–483. https://doi.org/10.1002/2014ms000344

Teodoru, C. R., Del Giorgio, P. A., Prairie, Y. T., & St-Pierre, A. (2013). Depositional fluxes and sources of particulate carbon and nitrogen in natural lakes and a young boreal reservoir in Northern Québec. *Biogeochemistry*, *113*(1–3), 323–339. https://doi.org/10.1007/s10533-012-9760-x

Tremblay, A., Varfalvy, C.L., Roehm, M., & Garneau (Eds.) (2005). *Greenhouse gas emissions—Fluxes and processes*. Springer.

Utsumi, M., Nojiri, Y., Nakamura, T., Nozawa, T., Otsuki, A., Takamura, N., et al. (1998). Dynamics of dissolved methane and methane oxidation in dimictic Lake Nojiri during winter. *Limnology and Oceanography*, *43*(1), 10–17. https://doi.org/10.4319/lo.1998.43.1.0010

Vachon, D., Prairie, Y. T., Guillemette, F., & Del Giorgio, P. A. (2017). Modeling allochthonous dissolved organic carbon mineralization under variable hydrologic regimes in boreal lakes. *Ecosystems*, *20*(4), 781–795. https://doi.org/10.1007/s10021-016-0057-0

Van Coillie, R., Visser, S. A., Campbell, P. G. C., & Jones, H. G. (1983). A study of the breakdown of wood of conifers submerged for over half a century in a reservoir. *Annales de Limnologie*, *19*(2), 129–134. https://doi.org/10.1051/limn/1983014

Varon, D. J., McKeever, J., Jervis, D., Maasakkers, J. D., Pandey, S., Houweling, S., et al. (2019). Satellite discovery of anomalously large methane point sources from oil/gas production. *Geophysical Research Letters*, *46*(22), 13507–13516. https://doi.org/10.1029/2019GL083798

Veefkind, J. P., Aben, I., McMullan, K., Förster, H., de Vries, J., Otter, G., et al. (2012). TROPOMI on the ESA sentinel-5 precursor: A GMES mission for global observations of the atmospheric composition for climate, air quality and ozone layer applications. *Remote Sensing of Environment*, *120*, 70–83. https://doi.org/10.1016/j.rse.2011.09.027

Venkiteswaran, J. J., Schiff, S. L., St. Louis, V. L., Matthews, C. J. D., Boudreau, N. M., Joyce, E. M., et al. (2013). Processes affecting greenhouse gas production in experimental boreal reservoirs. *Global Biogeochemical Cycles*, *27*(2), 567–577. https://doi.org/10.1002/gbc.20046

Venkiteswaran, J. J., Wassenaar, L. I., & Schiff, S. L. (2007). Dynamics of dissolved oxygen isotopic ratios: A transient model to quantify primary production, community respiration, and air–water exchange in aquatic ecosystems. *Oecologia*, *153*(2), 385–398. https://doi.org/10.1007/s00442-007-0744-9

Wachenfeldt, E. V., Bastviken, D., & Tranvika, L. J. (2009). Microbially induced flocculation of allochthonous dissolved organic carbon in lakes. *Limnology and Oceanography*, *54*(5), 1811–1818. https://doi.org/10.4319/lo.2009.54.5.1811

Walter, K. M., Zimov, S. A., Chanton, J. P., Verbyla, D., & Chapin, F. S., 3rd. (2006). Methane bubbling from Siberian thaw lakes as a positive feedback to climate warming. *Nature*, *443*(7107), 71–75. https://doi.org/10.1038/nature05040

West, W. E., Creamer, K. P., & Jones, S. E. (2016). Productivity and depth regulate lake contributions to atmospheric methane. *Limnology and Oceanography*, *61*(S1), S51–S61. https://doi.org/10.1002/lno.10247

Wetzel, R. (2001). *Limnology: Lake and river ecosystems* (Vol. 3). Academic Press.

Wik, M., Thornton, B. F., Bastviken, D., Uhlbäck, J., & Crill, P. M. (2016). Biased sampling of methane release from northern lakes: A problem for extrapolation. *Geophysical Research Letters*, *43*(3), 1256–1262. https://doi.org/10.1002/2015gl066501

Winton, R. S., Calamita, E., & Wehrli, B. (2019). Reviews and syntheses: Dams, water quality and tropical reservoir stratification. *Biogeosciences*, *16*(8), 1657–1671. https://doi.org/10.5194/bg-16-1657-2019

Yao, M., Henny, C., & Maresca, J. A. (2016). Freshwater Bacteria release methane as a by-product of phosphorus acquisition. *Applied and Environmental Microbiology*, *82*(23), 6994–7003. https://doi.org/10.1128/AEM.02399-16

Yigzaw, W., Li, H.-Y., Fang, X., Leung, L. R., Voisin, N., Hejazi, M. I., & Demissie, Y. (2019). A multilayer reservoir thermal stratification module for earth system models. *Journal of Advances in Modeling Earth Systems*, *11*(10), 3265–3283. https://doi.org/10.1029/2019MS001632

Zarfl, C., Lumsdon, A. E., Berlekamp, J., Tydecks, L., & Tockner, K. (2015). A global boom in hydropower dam construction. *Aquatic Sciences*, *77*(1), 161–170. https://doi.org/10.1007/s00027-014-0377-0

Zhang, H., Chen, G., Hu, J., Chen, S.-H., Wiedinmyer, C., Kleeman, M., & Ying, Q. (2014). Evaluation of a seven-year air quality simulation using the Weather Research and Forecasting (WRF)/Community Multiscale Air Quality (CMAQ) models in the eastern United States. *The Science of the Total Environment*, *473–474*, 275–285. https://doi.org/10.1016/j.scitotenv.2013.11.121

Zhou, Y., Zhou, L., Zhang, Y., Garcia de Souza, J., Podgorski, D. C., Spencer, R. G. M., et al. (2019). Autochthonous dissolved organic matter potentially fuels methane ebullition from experimental lakes. *Water Research*, *166*, 115048. https://doi.org/10.1016/j.watres.2019.115048

References From the Supporting Information

Alves, B. G. T. A., & Bertolino, S. M. (2016). *Estudo du grau de trofia da represa de Miranda-mg*. XIII Congresso Nacional de Meio Ambiente de Pocos de Caldas.

Araújo, C. A. S., Sampaio, F. G., Alcântara, E., Curtarelli, M. P., Ogashawara, I., & Stech, J. L. (2017). Effects of atmospheric cold fronts on stratification and water quality of a tropical reservoir: Implications for aquaculture. *Aquaculture Environment Interactions*, *9*, 385–403. https://doi.org/10.3354/aei00240

Araújo, F. G., Morado, C. N., Parente, T. T. E., Paumgartten, F. J. R., & Gomes, I. D. (2017). Biomarkers and bioindicators of the environmental condition using a fish species (Pimelodus maculatus Lacepède, 1803) in a tropical reservoir in Southeastern Brazil. *Brazilian Journal of Biology*, *78*(2), 351–359. https://doi.org/10.1590/1519-6984.167209

Beilfuss, R. (2010). Modelling trade-offs between hydropower generation and environmental flow scenarios: A case study of the Lower Zambezi River Basin, Mozambique. *International Journal of River Basin Management*, *8*(3–4), 331–347. https://doi.org/10.1080/15715124.2010.533643

Bergier, I., Evlyn, M. L., Ramos, F. M., Mazzi, E. A., & Maria, F. F. (2011). Carbon dioxide and methane fluxes in the littoral zone of a tropical savanna reservoir (Corumbá, Brazil). *Oecologia Australis*, *15*(3), 666–681. https://doi.org/10.4257/oeco.2011.1503.17

Bernardo, J. W. Y., Mannich, M., Hilgert, S., Fernandes, C. V. S., & Bleninger, T. (2017). A method for the assessment of long-term changes in carbon stock by construction of a hydropower reservoir. *Ambio*, *46*(5), 566–577. https://doi.org/10.1007/s13280-016-0874-6

Bevelhimer, M. S., Stewart, A. J., Fortner, A. M., Phillips, J. R., & Mosher, J. J. (2016). CO_2 is dominant greenhouse gas emitted from six hydropower reservoirs in southeastern United States during peak summer emissions. *Water*, *8*(1), 15. https://doi.org/10.3390/w8010015

Borges, P. A. F., Train, S., & Rodrigues, L. C. (2008). Spatial and temporal variation of phytoplankton in two subtropical Brazilian reservoirs. *Hydrobiologia*, *607*(1), 63–74. https://doi.org/10.1007/s10750-008-9367-3

Brothers, S. M., del Giorgio, P. A., Teodoru, C. R., & Prairie, Y. T. (2012). Landscape heterogeneity influences carbon dioxide production in a young boreal reservoir. *Canadian Journal of Fisheries and Aquatic Sciences*, *69*(3), 447–456. https://doi.org/10.1139/f2011-174

Bunting, L., Leavitt, P. R., Simpson, G. L., Wissel, B., Laird, K. R., Cumming, B. F., et al. (2016). Increased variability and sudden ecosystem state change in lake Winnipeg, Canada, caused by 20th century agriculture: Lake Winnipeg variability and state change. *Limnology and Oceanography*, *61*(6), 2090–2107. https://doi.org/10.1002/lno.10355

Calijuri, M. C., & Dos Santos, A. C. A. (2001). Temporal variations in phytoplankton primary production in a tropical reservoir (Barra Bonita, SP-Brazil). *Hydrobiologia*, *445*(1), 11–26. https://doi.org/10.1023/A:1017554829992

Chanudet, V., Gaillard, J., Lambelain, J., Demarty, M., Descloux, S., Félix-Faure, J., et al. (2020). Emission of greenhouse gases from French temperate hydropower reservoirs. *Aquatic Sciences*, *82*(3), 51. https://doi.org/10.1007/s00027-020-00721-3

Cunha, D. G. F., Benassi, S. F., de Falco, P. B., & do Carmo Calijuri, M. (2016). Trophic state evolution and nutrient trapping capacity in a transboundary subtropical reservoir: A 25-year study. *Environmental Management*, *57*(3), 649–659. https://doi.org/10.1007/s00267-015-0633-7

de Junet, A., Abril, G., Guérin, F., Billy, I., & de Wit, R. (2009). A multi-tracers analysis of sources and transfers of particulate organic matter in a tropical reservoir (Petit Saut, French Guiana). *River Research and Applications*, *25*(3), 253–271. https://doi.org/10.1002/rra.1152

de Mello, N. A. S. T., Brighenti, L. S., Barbosa, F. A. R., Staehr, P. A., & Bezerra Neto, J. F. (2018). Spatial variability of methane (CH_4) ebullition in a tropical hypereutrophic reservoir: Silted areas as a bubble hot spot. *Lake and Reservoir Management*, *34*(2), 105–114. https://doi.org/10.1080/10402381.2017.1390018

De Lima, I. B. T., de Moraes Novo, E. M. L., Ballester, M. V. R., & Ometto, J. P. (1998). Methane production, transport and emission in Amazon hydroelectric plants. IGARSS '98. In *Sensing and Managing the Environment. 1998 IEEE International Geoscience and Remote Sensing. Symposium proceedings. (Cat. No.98CH36174)* (Vol. 5, pp. 2529–2531). https://doi.org/10.1109/IGARSS.1998.702268

DelSontro, T., McGinnis, D. F., Sobek, S., Ostrovsky, I., & Wehrli, B. (2010). Extreme methane emissions from a Swiss hydropower reservoir: Contribution from bubbling sediments. *Environmental Science & Technology*, *44*(7), 2419–2425. https://doi.org/10.1021/es9031369

Demarty, M., Bastien, J., & Tremblay, A. (2011). Annual follow-up of gross diffusive carbon dioxide and methane emissions from a boreal reservoir and two nearby lakes in Québec, Canada. *Biogeosciences*, *8*(1), 41–53. https://doi.org/10.5194/bg-8-41-2011

Demarty, M., Bastien, J., Tremblay, A., Hesslein, R. H., & Gill, R. (2009). Greenhouse gas emissions from boreal reservoirs in Manitoba and Québec, Canada, measured with automated systems. *Environmental Science & Technology*, *43*(23), 8908–8915. https://doi.org/10.1021/es8035658

Descloux, S., Chanudet, V., Serça, D., & Guérin, F. (2017). Methane and nitrous oxide annual emissions from an old eutrophic temperate reservoir. *The Science of the Total Environment*, *598*, 959–972. https://doi.org/10.1016/j.scitotenv.2017.04.066

Deshmukh, C., Serça, D., Delon, C., Tardif, R., Demarty, M., Jarnot, C., et al. (2014). Physical controls on CH_4 emissions from a newly flooded subtropical freshwater hydroelectric reservoir: Nam Theun 2. *Biogeosciences*, *11*(15), 4251–4269. https://doi.org/10.5194/bg-11-4251-2014

Diem, T., Koch, S., Schwarzenbach, S., Wehrli, B., & Schubert, C. J. (2012). Greenhouse gas emissions (CO_2, CH_4, and N_2O) from several perialpine and alpine hydropower reservoirs by diffusion and loss in turbines. *Aquatic Sciences*, *74*(3), 619–635. https://doi.org/10.1007/s00027-012-0256-5

Domingues, C. D., da Silva, L. H. S., Rangel, L. M., de Magalhães, L., de Melo Rocha, A., Lobão, L. M., et al. (2017). Microbial food-web drivers in tropical reservoirs. *Microbial Ecology*, *73*(3), 505–520. https://doi.org/10.1007/s00248-016-0899-1

dos Santos, M. A., Rosa, L. P., Sikar, B., Sikar, E., & dos Santos, E. O. (2006). Gross greenhouse gas fluxes from hydro-power reservoir compared to thermo-power plants. *Energy Policy*, *34*(4), 481–488. https://doi.org/10.1016/j.enpol.2004.06.015

Duchemin, E., Lucotte, M., Canuel, R., & Chamberland, A. (1995). Production of the greenhouse gases CH_4 and CO_2 by hydroelectric reservoirs of the boreal region. *Global Biogeochemical Cycles*, *9*(4), 529–540. https://doi.org/10.1029/95GB02202

Duchemin, E., Lucotte, M., Canuel, R., Queiroz, A. G., Almeida, D. C., Pereira, H. C., & Dezincourt, J. (2000). Comparison of greenhouse gas emissions from an old tropical reservoir with those from other reservoirs worldwide. *Internationale Vereinigung für Theoretische und Angewandte Limnologie: Verhandlungen*, *27*(3), 1391–1395. https://doi.org/10.1080/03680770.1998.11901464

Dumestre, J. F., Casamayor, E. O., Massana, R., & Pedrós-Alió, C. (2002). Changes in bacterial and archaeal assemblages in an equatorial river induced by the water eutrophication of Petit Saut dam reservoir (French Guiana). *Aquatic Microbial Ecology: International Journal*, *26*, 209–221. https://doi.org/10.3354/ame026209

Filatov, N., & Rukhovets, L. (2012). Ladoga Lake and Onego Lake (Lakes Ladozhskoye and Onezhskoye). *Encyclopedia of Earth Sciences Series*, 429–432. https://doi.org/10.1007/978-1-4020-4410-6_197

Gikas, G. D., Tsihrintzis, V. A., Akratos, C. S., & Haralambidis, G. (2009). Water quality trends in polyphytos reservoir, aliakmon river, Greece. *Environmental Monitoring and Assessment*, *149*(1–4), 163–181. https://doi.org/10.1007/s10661-008-0191-z

Grönlund, E., & Viljanen, M. (2003). Comparison of automatic and conventional physical and chemical analyses in Lake Saimaa, Eastern Finland. *Hydrobiologia*, *506–509*(1–3), 59–65. https://doi.org/10.1023/b:hydr.0000008559.29601.f0

Gruca-Rokosz, R. (2020). Quantitative fluxes of the greenhouse gases CH_4 and CO_2 from the surfaces of selected polish reservoirs. *Atmosphere*, *11*(3), 286. https://doi.org/10.3390/atmos11030286

Guérin, F., Abril, G., Richard, S., Burban, B., Reynouard, C., Seyler, P., & Delmas, R. (2006). Methane and carbon dioxide emissions from tropical reservoirs: Significance of downstream rivers. *Geophysical Research Letters*, *33*, L21407. https://doi.org/10.1029/2006gl027929

Hardenbicker, P., Rolinski, S., Weitere, M., & Fischer, H. (2014). Contrasting long-term trends and shifts in phytoplankton dynamics in two large rivers: Long-term phytoplankton dynamics. *International Review of Hydrobiology*, *99*(4), 287–299. https://doi.org/10.1002/iroh.201301680

Harrison, J. A., Deemer, B. R., Birchfield, M. K., & O'Malley, M. T. (2017). Reservoir water-level drawdowns accelerate and amplify methane emission. *Environmental Science & Technology*, *51*(3), 1267–1277. https://doi.org/10.1021/acs.est.6b03185

Heikal, M. (2010). Impact of water level fluctuation on water quality and trophic state of Lake Nasser and its khors, Egypt. *Egyptian Journal of Aquatic Biology and Fisheries*, *14*(1), 75–86. https://doi.org/10.21608/ejabf.2010.2054

Hilgert, S., Fernandes, C. V. S., & Fuchs, S. (2019). Redistribution of methane emission hot spots under drawdown conditions. *The Science of the Total Environment*, *646*, 958–971. https://doi.org/10.1016/j.scitotenv.2018.07.338

Huttunen, J. T., Väisänen, T. S., Hellsten, S. K., Heikkinen, M., Nykänen, H., Jungner, H., et al. (2002). Fluxes of CH_4, CO_2, and N_2O in hydroelectric reservoirs Lokka and Porttipahta in the northern boreal zone in Finland. *Global Biogeochemical Cycles*, *16*(1), 3–3-17. https://doi.org/10.1029/2000GB001316

Johnson, D. M. (1985). *Atlas of Oregon Lakes*. Oregon State University Press.

Joyce, J., & Jewell, P. W. (2003). Physical controls on methane ebullition from reservoirs and lakes. *Environmental and Engineering Geoscience*, *9*(2), 167–178. https://doi.org/10.2113/9.2.167

Karikari, A. Y., Akpabey, F., & Abban, E. K. (2013). Assessment of water quality and primary productivity characteristics of Volta Lake in Ghana. *Academia Journal of Environmental Sciences*, *1*(5), 88–103. https://doi.org/10.15413/ajes.2012.0109

Kasper, D., Forsberg, B. R., Amaral, J. H. F., Leitão, R. P., Py-Daniel, S. S., Bastos, W. R., & Malm, O. (2014). Reservoir stratification affects methylmercury levels in river water, plankton, and fish downstream from Balbina hydroelectric dam, Amazonas, Brazil. *Environmental Science & Technology*, *48*(2), 1032–1040. https://doi.org/10.1021/es4042644

Kehrig, H. A., Palermo, E. F. A., Seixas, T. G., Santos, H. S. B., Malm, O., & Akagi, H. (2009). Methyl and total mercury found in two man-made Amazonian reservoirs. *Journal of the Brazilian Chemical Society*, *20*(6), 1142–1152. https://doi.org/10.1590/s0103-50532009000600021

Keller, M., & Stallard, R. F. (1994). Methane emission by bubbling from Gatun lake, Panama. *Journal of Geophysical Research*, *99*(D4), 8307. https://doi.org/10.1029/92jd02170

Kelly, C. A., Rudd, J. W. M., St. Louis, V. L., & Moore, T. (1994). Turning attention to reservoir surfaces, a neglected area in greenhouse studies. *Eos, Transactions American Geophysical Union*, *75*(29), 332. https://doi.org/10.1029/94eo00987

King, A. (2018). "Priest rapids dam on columbia river Leaking in several sections". Northwest public Broadcasting. Retrieved from https://www.nwpb.org/2018/04/10/priest-rapids-dam-leaking-in-several-sections/

Kunz, M. J., Anselmetti, F. S., Wüest, A., Wehrli, B., Vollenweider, A., Thüring, S., & Senn, D. B. (2011). Sediment accumulation and carbon, nitrogen, and phosphorus deposition in the large tropical reservoir Lake Kariba (Zambia/Zimbabwe). *Journal of Geophysical Research*, *116*(G3), G03003. https://doi.org/10.1029/2010jg001538

Lieberman, D. M., & Grabowski, S. J. (2007). Physical, Chemical, and Biological Characteristics of Cle Elum and Bumping Lakes in the Upper Yakima River Basin, Storage Dam Fish Passage Study, Yakima Project, Washington, Technical Series No. PN-YDFP-005, Bureau of reclamation, Boise, Idaho, March 2007.

Lima, I. B. T. (2005). Biogeochemical distinction of methane releases from two Amazon hydroreservoirs. *Chemosphere*, *59*(11), 1697–1702. https://doi.org/10.1016/j.chemosphere.2004.12.011

Lima, I. B. T., Victoria, R. L., Novo, E. M. L. M., Feigl, B. J., Ballester, M. V. R., & Ometto, J. P. (2002). Methane, carbon dioxide and nitrous oxide emissions from two Amazonian reservoirs during high water table. *SIL Proceedings*, *28*(1), 438–442. https://doi.org/10.1080/03680770.2001.11902620

Lower Monumental Lock and Dam. (2021). US Army Corps of Engineers, Walla Walla District Website. Retrieved from https://www.nww.usace.army.mil/Locations/District-Locks-and-Dams/Lower-Monumental-Lock-and-Dam/

Marcelino, A. A., Santos, M. A., Xavier, V. L., Bezerra, C. S., Silva, C. R. O., Amorim, M. A., et al. (2015). Diffusive emission of methane and carbon dioxide from two hydropower reservoirs in Brazil. *Brazilian Journal of Biology*, *75*(2), 331–338. https://doi.org/10.1590/1519-6984.12313

Matsumura-Tundisi, T., Tundisi, J. G., Tundisi, M. E. J., & Cimbleris, A. (2006). Carbon content and composition of zooplankton fractions in two reservoirs of Central Brazil: Serra da Mesa and Manso. *Internationale Vereinigung für theoretische und angewandte Limnologie: Verhandlungen*, *29*(5), 2237–2244. https://doi.org/10.1080/03680770.2006.11903089

Miller, B. L., Arntzen, E. V., Goldman, A. E., & Richmond, M. C. (2017). Methane ebullition in temperate hydropower reservoirs and implications for US policy on greenhouse gas emissions. *Environmental Management*, *60*(4), 615–629. https://doi.org/10.1007/s00267-017-0909-1

Mineeva, N. M., Semadeny, I. V., & Makarova, O. S. (2020). Chlorophyll content and the modern trophic state of the Volga River reservoirs (2017–2018). *Inland Water Biology*, *13*(2), 327–330. https://doi.org/10.1134/s199508292002008x

Montgomery, S., Lucotte, M., Pichet, P., & Mucci, A. (1995). Total dissolved mercury in the water column of several natural and artificial aquatic systems of Northern Quebec (Canada). *Canadian Journal of Fisheries and Aquatic Sciences*, *52*(11), 2483–2492. https://doi.org/10.1139/f95-839

Mosher, J. J., Fortner, A. M., Phillips, J. R., Bevelhimer, M. S., Stewart, A. J., & Troia, M. J. (2015). Spatial and temporal correlates of greenhouse gas diffusion from a hydropower reservoir in the southern United States. *Water*, *7*(11), 5910–5927. https://doi.org/10.3390/w7115910

Nanini-Costa, M. H., Quináglia, G. A., Petesse, M. L., & Esteves, K. E. (2017). Diet of an invading clupeid along an urban neotropical reservoir: Responses to different environmental conditions. *Environmental Biology of Fishes*, *100*(10), 1193–1212. https://doi.org/10.1007/s10641-017-0636-8

Ogashawara, I., Alcântara, E., Curtarelli, M., Adami, M., Nascimento, R., Souza, A., et al. (2014). Performance analysis of MODIS 500-m spatial resolution products for estimating chlorophyll-*a* concentrations in oligo-to meso-trophic waters case study: Itumbiara reservoir, Brazil. *Remote Sensing*, *6*(2), 1634–1653. https://doi.org/10.3390/rs6021634

Ometto, J. P., Cimbleris, A. C. P., dos Santos, M. A., Rosa, L. P., Abe, D., Tundisi, J. G., et al. (2013). Carbon emission as a function of energy generation in hydroelectric reservoirs in Brazilian dry tropical biome. *Energy Policy*, *58*, 109–116. https://doi.org/10.1016/j.enpol.2013.02.041

Pacheco, F. S., Soares, M. C. S., Assireu, A. T., Curtarelli, M. P., Roland, F., Abril, G., et al. (2015). The effects of river inflow and retention time on the spatial heterogeneity of chlorophyll and water-air CO_2 fluxes in a tropical hydropower reservoir. *Biogeosciences*, *12*(1), 147–162. https://doi.org/10.5194/bg-12-147-2015

Poletaeva, V. I., Pastukhov, M. V., Zagorulko, N. A., & Belogolova, G. A. (2018). Changes in water hydrochemistry in bays of the Bratsk reservoir caused by forest harvesting operations. *Water Resources*, *45*(3), 369–378. https://doi.org/10.1134/s0097807818030119

Rawson, D. S. (1960). A limnological comparison of twelve large lakes in northern Saskatchewan. *Limnology & Oceanography*, *195*(2), 212–211. https://doi.org/10.4319/lo.1960.5.2.0195

Rodriguez, M., & Casper, P. (2018). Greenhouse gas emissions from a semi-arid tropical reservoir in northeastern Brazil. *Regional Environmental Change*, *18*(7), 1901–1912. https://doi.org/10.1007/s10113-018-1289-7

Rogério, J. P., Santos, M. A., & Santos, E. O. (2013). Influence of environmental variables on diffusive greenhouse gas fluxes at hydroelectric reservoirs in Brazil. *Brazilian Journal of Biology = Revista Brasleira de Biologia*, *73*(4), 753–764. https://doi.org/10.1590/s1519-69842013000400011

Roland, F., Vidal, L. O., Pacheco, F. S., Barros, N. O., Assireu, A., Ometto, J. P. H. B., et al. (2010). Variability of carbon dioxide flux from tropical (Cerrado) hydroelectric reservoirs. *Aquatic Sciences*, *72*(3), 283–293. https://doi.org/10.1007/s00027-010-0140-0

Rosa, L. P., dos Santos, M. A., Matvienko, B., dos Santos, E. O., & Sikar, E. (2004). Greenhouse gas emissions from hydroelectric reservoirs in tropical regions. *Climatic Change*, *66*(1/2), 9–21. https://doi.org/10.1023/b:clim.0000043158.52222.ee

Rosa, L. P., Dos Santos, M. A., Matvienko, B., Sikar, E., Lourenço, R. S. M., & Menezes, C. F. (2003). Biogenic gas production from major Amazon reservoirs, Brazil. *Hydrological Processes*, *17*(7), 1443–1450. https://doi.org/10.1002/hyp.1295

Samiotis, G., Pekridis, G., Kaklidis, N., Trikoilidou, E., Taousanidis, N., & Amanatidou, E. (2018). Greenhouse gas emissions from two hydroelectric reservoirs in Mediterranean region. *Environmental Monitoring and Assessment*, *190*(6), 363. https://doi.org/10.1007/s10661-018-6721-4

Silva, L. C. D., Leone, I. C., Santos-Wisniewski, M. J. D., Peret, A. C., & Rocha, O. (2012). Invasion of the dinoflagellate Ceratium furcoides (Levander) Langhans 1925 at tropical reservoir and its relation to environmental variables. *Biota Neotropica*, *12*(2), 93–100. https://doi.org/10.1590/S1676-06032012000200010

St. Louis, V. L., Kelly, C. A., Duchemin, É., Rudd, J. W. M., & Rosenberg, D. M. (2000). Reservoir surfaces as sources of greenhouse gases to the atmosphere: A global estimate: Reservoirs are sources of greenhouse gases to the atmosphere, and their surface areas have increased to the point where they should be included in global inventories of anthropogenic emissions of greenhouse gases. *BioScience*, *50*(9), 766–775. https://doi.org/10.1641/0006-3568(2000)050[0766:RSASOG]2.0.CO;2

Tadonléké, R. D., Marty, J., & Planas, D. (2012). Assessing factors underlying variation of CO_2 emissions in boreal lakes vs. reservoirs. *FEMS Microbiology Ecology*, *79*(2), 282–297. https://doi.org/10.1111/j.1574-6941.2011.01218.x

Teodoru, C. R., Bastien, J., Bonneville, M.-C., del Giorgio, P. A., Demarty, M., Garneau, M., et al. (2012). The net carbon footprint of a newly created boreal hydroelectric reservoir. *Global Biogeochemical Cycles*, *26*(2), GB2016. https://doi.org/10.1029/2011GB004187

Teodoru, C. R., Nyoni, F. C., Borges, A. V., Darchambeau, F., Nyambe, I., & Bouillon, S. (2015). Dynamics of greenhouse gases (CO_2, CH_4, N_2O) along the Zambezi River and major tributaries, and their importance in the riverine carbon budget. *Biogeosciences*, *12*(8), 2431–2453. https://doi.org/10.5194/bg-12-2431-2015

Therrien, J., Tremblay, A., & Jacques, R. B. (2005). In A. Tremblay, L. Varfalvy, C. Roehm, & M. Garneau (Eds.), *Greenhouse gas emissions-fluxes and processes: Hydroelectric reservoirs and natural environments*. Springer.

Thornton, J. A. (1987). A review of some unique aspects of the limnology of shallow Southern African man-made lakes. *Geojournal*, *14*(3), 339–352. https://doi.org/10.1007/bf00208207

Tremblay, A., Therrien, J., Hamlin, B., Wichmann, E., & LeDrew, L. J. (2005). In A. Tremblay, L. Varfalvy, C. Roehm, & M. Garneau (Eds.), *Greenhouse gas emissions—Fluxes and processes hydroelectric reservoirs and natural environments* (pp. 209–232). Springer.

Vono, V., Silva, L. G. M., Maia, B. P., & Godinho, H. P. (2002). Biologia reprodutiva de três espécies simpátricas de peixes neotropicais: Pimelodus maculatus Lacépede (siluriformes, pimelodidae), Leporinus amblyrhynchus Garavello & Britski e Schizodon nasutus kner (characiformes, anostomidae) do recém-formado reservatório de Miranda, alto paraná. *Revista Brasileira de Zoologia*, *19*(3), 819–826. https://doi.org/10.1590/S0101-81752002000300020

Vörösmarty, C. J., Meybeck, M., Fekete, B., Sharma, K., Green, P., & Syvitski, J. P. M. (2003). Anthropogenic sediment retention: Major global impact from registered river impoundments. *Global and Planetary Change*, *39*(1), 169–190. https://doi.org/10.1016/S0921-8181(03)00023-7

Weissenberger, S., Lucotte, M., & Canuel, R. (2012). The carbon cycle of Quebec boreal reservoirs investigated by elemental compositions and isotopic values. *Biogeochemistry*, *111*(1–3), 555–568. https://doi.org/10.1007/s10533-011-9687-7

Wilander, A., & Persson, G. (2001). Recovery from eutrophication: Experiences of reduced phosphorus input to the four largest lakes of Sweden. *Ambio*, *30*(8), 475–485. https://doi.org/10.1579/0044-7447-30.8.475

Wilkinson, J., Bodmer, P., & Lorke, A. (2019). Methane dynamics and thermal response in impoundments of the Rhine River, Germany. *The Science of the Total Environment*, *659*, 1045–1057. https://doi.org/10.1016/j.scitotenv.2018.12.424